mDC TICAM-1 pathway efficiently links CTL/NK activation by mDCs. Missing the cell surface-specific TLR, TLR22, and conserving ER-resident TLR, TLR3, in mDCs may cause the functional specialization of the TICAM-1 pathway on evoking cellular immunity in mammals. Although the signaling pathway by which type I IFN is induced has been elucidated in each cell type, the exact pathway that drives NK activation or CTL induction by mDCs has not been identified.

Effector induction in transgenic mice with TLR22 for surface dsRNA recognition

Upon transfection of fgTLR22 or fgTLR3 into human or mouse cells, fgTLR22 functions as an RNA sensor for IFN induction in these mammalian cells, suggesting that mice and human TICAM-1 are compatible with fish TLR22 and TLR3 (37). With this finding in mind, we have generated TLR22 transgenic (Tg) mice to test fish TLR22 antiviral function and NK activation in mouse. TLR22 is ubiquitously expressed in all the organs tested in the Tg mice (A. Matsuo, H. Oshiumi, T. Seya, unpublished data). Its expression profile is similar to that in fish, in which endogenous fish TICAM-1 is ubiquitously expressed. PolyI:C or poliovirus were used as type I IFN inducers for *in vitro* mouse embryonic fibroblasts (MEF) stimulation studies. TLR22-expressing MEFs produce high levels of type I IFN within 6 h, a time period during which control MEFs still do not produce type I IFN. Rapid induction and three- to fivefold higher levels of IFN-β in the supernatant are characteristic features of TLR22-expressing MEFs. Similar results were obtained with BMDCs.

The levels of NK activation induced by BMDCs do not differ significantly between TLR22-expressing BMDCs and control BMDCs. We believe that TLR22 differs from TLR3 in its ability to activate cellular immune responses. However, further investigation is necessary to establish the final conclusion.

Virus infection studies were performed on Tg mice using influenza virus and poliovirus in an *in vivo* mouse model (A. Matsuo, H. Oshiumi, T. Seya, unpublished data). Both Tg and control mice died of influenza infection within 7 days. It appeared that TLR22 did not protect mice from influenza. By contrast, Tg mice expressing the poliovirus receptor (PVR) and TLR22 were relatively resistant to poliovirus infection compared with TLR22-negative control PVR-Tg mice. Wildtype mice died within 5 days, but Tg mice survived for a significant longer period. Hence, TLR22 harbors antiviral activity against acute infection of dsRNA or positive-stranded RNA viruses. This TLR22 function is conserved in TLR22-positive cells of Tg mice. We support the interpretation that TLR22 is lost in mammals so that the TLR22 supplement recovers resistance to dsRNA-generating viruses. The summary of this issue on TLR22-Tg mice is illustrated in Fig. 6.

Although cell surface activation of TLR3 or TLR22 may not be associated with induction of cellular immunity, these molecules efficiently suppress acute viral infection by generating type I IFN. Development of the endosomal RNA recognition system in mDCs would be essential in mammals for enhancing the induction of cell-mediated and long-lasting immunity in viral infection. Although to what extent TLR22 participates in the induction of cellular immunity by virus infection remains largely unsettled, fish unequivocally develop the endosomal RNA recognition system involving TLR3. Cell surface RNA recognition by TLR3 exerts some toxic features (7, 53), which may facilitate limited usage of TLR3 on membrane surface. Part of the linking between TLRs and cellular immune responses should have been established before human and fish ancestors diverged.

Prototype of the vertebrate TLR system

The phylogenetic tree of vertebrate TLR family members strongly supports the notion that non-mammalian vertebrate TLRs emerged during the Cambrian period together with other mammalian TLRs (13, 14, 36, 49); thus, the human ancestor probably possessed both contemporary TLR subsets and those of non-mammalian vertebrates. Based on our knowledge of the functional coverage of vertebrate TLR family members, the expected TLR subsets that the vertebrate

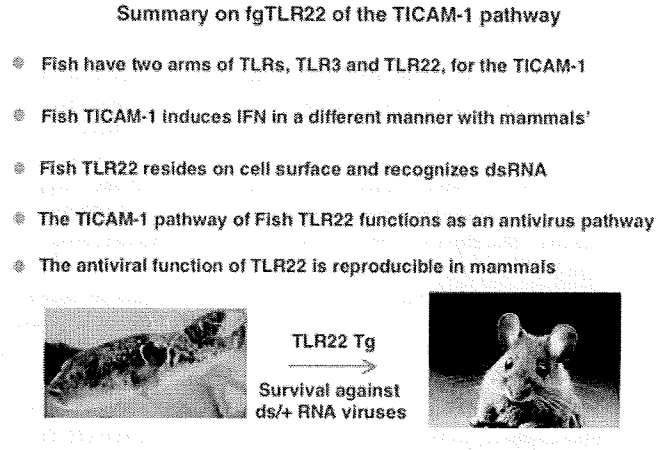

Fig. 6. Summary on fgTLR22 of the TICAM-1 pathway. (i) Fish have two arms of TLRs, TLR3, and TLR22, for the TICAM-1. (ii) Fish TICAM-1 induces IFN in a different manner with mammals. (iii) Fish TLR22 resides on cell surface and recognizes dsRNA. (iv) The TICAM-1 pathway of fish TLR22 functions as an antivirus pathway. (v) The antiviral function of TLR22 is reproducible in mammals.

common ancestor would have possessed would include at least the following 10 TLR members: TLR2, TLR3, TLR4, TLR5, TLR7, TLR8, TLR9, TLR21, TLR21, and TLR22 (13) (*Table* 1). Prior to the evolution of mammals, gene duplications would have occurred, especially in TLR2 subfamily members. Furthermore, some TLR genes were lost in some lineages, although the reason remains unknown. For example, TLR21 was diminished in the mammalian lineage, and TLR22 was lost when the mammalian ancestor began to live on land (36). Why did our human ancestor lose TLR21 and TLR22 during evolution? There are two possible explanations. First, mammals need to recognize patterns in the endosome to link the acquired responses so that non-mammalian TLRs present on the cell surface would become dispensable in the innate system. This scenario is conceivable, because the acquired system in mammals is far more sophisticated than that of teleosts. Second, the mammalian lineage happened to lose the non-mammalian TLRs. This observation is not surprising because loss of genes, which are useful for the descendant, has occurred occasionally during vertebrate evolution. For example, the vertebrate ancestor probably possessed broader spectral opsin genes for light sensing, keener auditory sensors for sound hearing, and more olfactory genes for smell sensing than humans, but the mammalian ancestor lost these outstanding genes since their divergence from reptiles (54); thus, many mammalian species are less sensitive to distal light wavelength of light, high frequency of sound, and faint smell than other non-mammalian vertebrates. If mammals had successfully reproduced TLR22 in their genomes, innate immunity in humans would have been stronger. Optional environmental pressure by pathogens may have led to the divergence of the immune system, resulting in variations. In any case, TLRs linked cellular immunity a long time ago: a common ancestor of fish and human already had a prototype. Based on this view, it appears that our immune system is not ideal but is just an example of how infections with certain pathogens have been prevented over a long time period.

References

1. Medzhitov R, Janeway CA Jr. Innate immunity: the virtues of a nonclonal system of recognition. Cell 1997;**91**:295–298.
2. Medzhitov R, Preston-Hurlburt P, Janeway CA Jr. A human homologue of the *Drosophila* Toll protein signals activation of adaptive immunity. Nature 1997;**388**:394–397.
3. Akira S, Uematsu S, Takeuchi O. Pathogen recognition and innate immunity. Cell 2006;**124**:783–801.
4. Yoneyama M, Fujita T. Function of RIG-I-like receptors in antiviral innate immunity. J Biol Chem 2007;**282**:15315–15318.
5. Matsumoto M, Seya T. TLR3: interferon induction by double-stranded RNA including poly(I:C). Adv Drug Deliv Rev 2008;**60**: 805–812.
6. Carter WA, Pitha PM, Marshall LW, Tazawa I, Tazawa S, Ts'o PO. Structural requirements of the rI n–rC n complex for induction of human interferon. J Mol Biol 1972;**70**:567–587.
7. Absher M, Stinebring WR. Toxic properties of a synthetic double-stranded RNA. Endotoxin-like properties of poly I:poly C, an interferon stimulator. Nature 1969; **223**:715–717.
8. Sasai M, Shingai M, Funami K, Yoneyama M, Fujita T, Matsumoto M, Seya T. NAK-associated protein 1 participates in both the TLR3 and the cytoplasmic pathways in type I IFN induction. J Immunol 2006;**177**: 8676–8683.
9. Honda K, Taniguchi T. IRFs: master regulators of signalling by Toll-like receptors and cytosolic pattern-recognition receptors. Nat Rev Immunol 2006;**6**:644–658.
10. Hoshino K, Kaisho T. Nucleic acid sensing Toll-like receptors in dendritic cells. Curr Opin Immunol 2008;**20**:408–413.
11. Iwasaki A, Medzhitov R. Toll-like receptor control of the adaptive immune responses. Nat Immunol 2004;**5**:987–995.
12. Reis e Sousa C. Dendritic cells in a mature age. Nat Rev Immunol 2006;**6**: 476–483.
13. Oshiumi H, Tsujita T, Shida K, Matsumoto M, Ikeo K, Seya T. Prediction of the prototype of the human Toll-like receptor gene family from the pufferfish, *Fugu rubripes*, genome. Immunogenetics 2003;**54**: 791–800.
14. Roach JC, et al. The evolution of vertebrate Toll-like receptors. Proc Natl Acad Sci USA 2005;**102**:9577–9582.
15. Baoprasertkul P, Peatman E, Somridhivej B, Liu Z. Toll-like receptor 3 and TICAM genes in catfish: species-specific expression profiles following infection with *Edwardsiella ictaluri*. Immunogenetics 2006;**58**:817–830.
16. Sullivan C, Postlethwait JH, Lage CR, Millard PJ, Kim CH. Evidence for evolving Toll-IL-1 receptor-containing adaptor molecule function in vertebrates. J Immunol 2007; **178**:4517–4527.
17. Yoneyama M, Onomoto K, Fujita T. Cytoplasmic recognition of RNA. Adv Drug Deliv Rev 2008;**60**:841–846.
18. Matsumoto M, et al. Subcellular localization of Toll-like receptor 3 in human dendritic cells. J Immunol 2003;**171**:3154–3162.
19. Ebihara T, Shingai M, Matsumoto M, Wakita T, Seya T. Hepatitis C virus-infected hepatocytes extrinsically modulate dendritic cell maturation to activate T cells and natural killer cells. Hepatology 2008;**48**: 48–58.
20. Fan S, et al. Zebrafish TRIF, a Golgi-localized protein, participates in IFN induction and NF-kappaB activation. J Immunol 2008;**180**:5373–5383.
21. Matsumoto M, Kikkawa S, Kohase M, Miyake K, Seya T. Establishment of a monoclonal antibody against human Toll-like receptor 3 that blocks double-stranded RNA-mediated signaling. Biochem Biophys Res Commun 2002;**293**:1364–1369.
22. Funami K, Matsumoto M, Oshiumi H, Akazawa T, Yamamoto A, Seya T. The cytoplasmic 'linker region' in Toll-like receptor 3 controls receptor localization and signaling. Int Immunol 2004;**16**:1143–1154.
23. de Bouteiller O, et al. Recognition of double-stranded RNA by human toll-like receptor 3 and downstream receptor signaling requires multimerization and an acidic pH. J Biol Chem 2005;**280**:38133–38145.
24. Oshiumi H, Matsumoto M, Funami K, Akazawa T, Seya T. TICAM-1, an adaptor molecule that participates in Toll-like receptor 3-mediated interferon-beta induction. Nat Immunol 2003;**4**:161–167.

25. Yamamoto M, et al. Role of adaptor TRIF in the MyD88-independent toll-like receptor signaling pathway. Science 2003;**301**: 640–643.
26. Häcker H, et al. Specificity in Toll-like receptor signalling through distinct effector functions of TRAF3 and TRAF6. Nature 2006;**439**:204–207.
27. Oganesyan G, et al. Critical role of TRAF3 in the Toll-like receptor-dependent and -independent antiviral response. Nature 2006;**439**:208–211.
28. Sharma S, tenOever BR, Grandvaux N, Zhou GP, Lin R, Hiscott J. Triggering the interferon antiviral response through an IKK-related pathway. Science 2003;**300**: 1148–1151.
29. Fitzgerald KA, et al. IKKepsilon and TBK1 are essential components of the IRF3 signaling pathway. Nat Immunol 2003;**4**:491–496.
30. Akazawa T, et al. Antitumor NK activation induced by the Toll-like receptor 3-TICAM-1 (TRIF) pathway in myeloid dendritic cells. Proc Natl Acad Sci USA 2007;**104**:252–257.
31. Schulz O, et al. Toll-like receptor 3 promotes cross-priming to virus-infected cells. Nature 2005;**433**:887–892.
32. Meylan E, Burns K, Hofmann K, Blancheteau V, Martinon F, Kelliher M, Tschopp J. RIP1 is an essential mediator of Toll-like receptor 3-induced NF-kappa B activation. Nat Immunol 2004;**5**:503–507.
33. Salem ML, Kadima AN, Cole DJ, Gillanders WE. Defining the antigen-specific T-cell response to vaccination and poly(I:C)/TLR3 signaling: evidence of enhanced primary and memory CD8 T-cell responses and antitumor immunity. J Immunother 2005;**28**: 220–228.
34. Sivori S, et al. CpG and double-stranded RNA trigger human NK cells by Toll-like receptors: induction of cytokine release and cytotoxicity against tumors and dendritic cells. Proc Natl Acad Sci USA 2004;**101**: 10116–10121.
35. Salaun B, Coste I, Rissoan MC, Lebecque SJ, Renno T. TLR3 can directly trigger apoptosis in human cancer cells. J Immunol 2006;**176**:4894–4901.
36. Oshiumi H, Matsuo A, Matsumoto M, Seya T. Pan-vertebrate Toll-like receptors during evolution. Curr Genomics 2008;**9**:488–493.
37. Matsuo A, et al. Teleost TLR22 recognizes RNA duplex to induce IFN and protect cells from birnaviruses. J Immunol 2008;**181**:3474–3485.
38. Funami K, Sasai M, Ohba Y, Oshiumi H, Seya T, Matsumoto M. Spatiotemporal mobilization of TICAM-1 in response to dsRNA. J Immunol 2007;**179**: 6827–6830.
39. Funami K, Sasai M, Oshiumi H, Seya T, Matsumoto M. Homo-oligomerization is essential for Toll/IL-1 receptor domain containing adaptor molecule-1 signaling. J Biol Chem 2008;**283**:18283–18291.
40. Bergan V, Steinsvik S, Xu H, Kileng Ø, Robertsen B. Promoters of type I interferon genes from Atlantic salmon contain two main regulatory regions. FEBS J 2006; **273**:3893–3906.
41. Rudd BD, et al. Deletion of TLR3 alters the pulmonary immune environment and mucus production during respiratory syncytial virus infection. J Immunol 2006; **176**:1937–1942.
42. Harada K, et al. Innate immune response to double-stranded RNA in biliary epithelial cells is associated with the pathogenesis of biliary atresia. Hepatology 2007;**46**: 1146–1154.
43. Cario E, Podolsky DK. Differential alteration in intestinal epithelial cell expression of toll-like receptor 3 (TLR3) and TLR4 in inflammatory bowel disease. Infect Immun 2000;**68**:7010–7017.
44. Nakamura MK, et al. Increased expression of TLR3 in human intrahepatic biliary epithelial cells at the site of ductular reaction in primary billiary cirrhosis. Hepatol Intern 2008;**2**:222–230.
45. Phelan PE, Pressley ME, Witten PE, Mellon MT, Blake S, Kim CH. Characterization of snakehead rhabdovirus infection in zebrafish (*Danio rerio*). J Virol 2005;**79**:1842–1852.
46. Nishizawa T, Kinoshita S, Yoshimizu M. An approach for genogrouping of Japanese isolates of aquabirnaviruses in a new genogroup, VII, based on the VP2/NS junction region. J Gen Virol 2005;**86**:1973–1978.
47. Ando T, Suzuki H, Nishimura S, Tanaka T, Hiraishi A, Kikuchi K. Characterization of extracellular RNAs produced by the marine photosynthetic bacterium *Rhodovulum sulfidophilum*. J Biochem 2006;**139**:805–811.
48. Coulibaly F, et al. The birnavirus crystal structure reveals structural relationships among icosahedral viruses. Cell 2005;**120**:761–772.
49. Ishii A, Kawasaki M, Matsumoto M, Tochinai S, Seya T. Phylogenetic and expression analysis of amphibian *Xenopus* Toll-like receptors. Immunogenetics 2007;**59**:281–293.
50. Akazawa T, et al. Tumor immunotherapy using bone marrow-derived dendritic cells overexpressing Toll-like receptor adaptors. FEBS Lett 2007;**581**:3334–3340.
51. Akazawa T, et al. Adjuvant-mediated tumor regression and tumor-specific cytotoxic response are impaired in MyD88-deficient mice. Cancer Res 2004;**64**:757–764.
52. Seya T, Akazawa T, Uehori J, Matsumoto M, Azuma I, Toyoshima K. Role of toll-like receptors and their adaptors in adjuvant immunotherapy for cancer. Anticancer Res 2003;**23**:4369–4376.
53. Zhou R, Wei H, Sun R, Tian Z. Recognition of double-stranded RNA by TLR3 induces severe small intestinal injury in mice. J Immunol 2007;**178**:4548–4556.
54. International Human Genome Sequencing Consortium. Finishing the euchromatic sequence of the human genome. Nature 2004;**431**:931–945.

THE JOURNAL OF BIOLOGICAL CHEMISTRY VOL. 284, NO. 2, pp. 807–817, January 9, 2009

Riplet/RNF135, a RING Finger Protein, Ubiquitinates RIG-I to Promote Interferon-β Induction during the Early Phase of Viral Infection*[S]

Received for publication, June 3, 2008, and in revised form, November 10, 2008 Published, JBC Papers in Press, November 18, 2008, DOI 10.1074/jbc.M804259200

Hiroyuki Oshiumi[‡], Misako Matsumoto[‡], Shigetsugu Hatakeyama[§], and Tsukasa Seya[‡1]

From the [‡]Department of Microbiology and Immunology and the [§]Department of Biochemistry, Hokkaido University Graduate School of Medicine, Kita-15, Nishi-7, Kita-ku Sapporo 060-8638, Japan

RIG-I (retinoic acid-inducible gene-I), a cytoplasmic RNA helicase, interacts with IPS-1/MAVS/Cardif/VISA, a protein on the outer membrane of mitochondria, to signal the presence of virus-derived RNA and induce type I interferon production. Activation of RIG-I requires the ubiquitin ligase, TRIM25, which mediates lysine 63-linked polyubiquitination of the RIG-I N-terminal CARD-like region. However, how this modification proceeds for activation of IPS-1 by RIG-I remains unclear. Here we identify an alternative factor, Riplet/RNF135, that promotes RIG-I activation independent of TRIM25. The Riplet/RNF135 protein consists of an N-terminal RING finger domain, C-terminal SPRY and PRY motifs, and shows sequence similarity to TRIM25. Immunoprecipitation analyses demonstrated that the C-terminal helicase and repressor domains of RIG-I interact with the Riplet/RNF135 C-terminal region, whereas the CARD-like region of RIG-I is dispensable for this interaction. Riplet/RNF135 promotes lysine 63-linked polyubiquitination of the C-terminal region of RIG-I, modification of which differs from the N-terminal ubiquitination by TRIM25. Overexpression and knockdown analyses revealed that Riplet/RNF135 promotes RIG-I-mediated interferon-β promoter activation and inhibits propagation of the negative-strand RNA virus, vesicular stomatitis virus. Our data suggest that Riplet/RNF135 is a novel factor of the RIG-I pathway that is involved in the evoking of human innate immunity against RNA virus infection, and activates RIG-I through ubiquitination of its C-terminal region. We infer that a variety of RIG-I-ubiquitinating molecular complexes sustain RIG-I activation to modulate RNA virus replication in the cytoplasm.

Cytoplasmic viral RNA sensors induce production of type I interferon (IFN)[2] (1, 2). Representative cytoplasmic sensors, RIG-I-like receptors (RLRs) of RIG-I, MDA5, and LGP2, belong to the DEA(D/H) box RNA helicase family (3–6). RIG-I recognizes the 5′ end triphosphate of the virus RNA genome or double-stranded RNA (6–8) to sense infection by various RNA viruses (3, 5). The RIG-I protein consists of two N-terminal CARD-like domains, an RNA helicase region and a repressor domain (RD) (9). After recognition of positive or negative single-stranded viral RNA, RIG-I interacts with its adaptor molecule IPS-1/MAVS/Cardif/VISA leading to type I IFN production, thereby protecting host cells from amplified viral replication (10–13). However, only a few copies of viral RNAs usually penetrate the cell membrane to enter the cell at an early infection, and these RLRs are barely present in intact as well as early virus-infected cells (6). The early viral RNA recognition facility should be different from that of the late phase when RIG-I protein is abundant in the cytoplasm and easily re-organizes the virus RNAs. What molecular mechanism is responsible for initial sensing of viral RNA thus remains unknown.

Other RLRs, MDA5 and LGP2, are structurally similar to RIG-I in their having the helicase domain (5, 14). However, MDA5 lacks the RD domain although it possesses CARD-like region at the N terminus like RIG-I. LGP2 does not have a CARD-like region but possesses RD at its C terminus (9). RIG-I and MDA5 recognize different kinds of RNA viruses and in some cases play a redundant role in sensing virus infection, such as influenza B (15). In contrast, LGP2 rather negatively regulates virus replication. LGP2 expression suppressed RIG-I or MDA5 signaling (14, 16), and *lgp2* gene disruption conferred high susceptibility to virus infection on mice (4).

Recently, the majority of proteins involved in the type I IFN-inducing system were found ubiquitinated. For example, the tumor necrosis factor receptor-associated family members, TRAF3 and TRAF6, are ubiquitin ligases to induce ubiquitination of proteins and implicated in activation of IFN regulatory factor (IRF) 3 or nuclear factor (NF) κB (13, 17–19). In contrast, a deubiquitinating enzyme, DUBA or A20, suppresses these signals (19, 20). In addition to ubiquitin, ubiquitin-like protein, ISG15, is also conjugated to proteins involved in the IFN-inducing pathway (21, 22). Recent studies have revealed that viral RNA sensors are also ubiquitinated. TRIM25 (ZNF147 or EFP), a member of the ubiquitin-protein isopeptide ligase family, which possesses a RING finger domain, ubiquitinates the

* This work was supported in part by grants-in-aid from the Ministry of Education, Science and Culture of Japan, Ministry of Health, Labour, and Welfare, The Mitsubishi Foundation, and The Mochida Memorial Foundation. The costs of publication of this article were defrayed in part by the payment of page charges. This article must therefore be hereby marked "*advertisement*" in accordance with 18 U.S.C. Section 1734 solely to indicate this fact.

[S] The on-line version of this article (available at http://www.jbc.org) contains supplemental Figs. S1–S6.

The nucleotide sequence(s) reported in this paper has been submitted to the GenBank™/EBI Data Bank with accession number(s) AB470605.

[1] To whom correspondence should be addressed: Dept. of Microbiology and Immunology, Graduate School of Medicine, Hokkaido University, Kita-ku, Sapporo 060-8638, Japan. Tel.: 81-11-706-5073; Fax: 81-11-706-7866; E-mail: seya-tu@pop.med.hokudai.ac.jp.

[2] The abbreviations used are: IFN, interferon; RT, reverse transcription; RLR, RIG-I-like receptor; HA, hemagglutinin; siRNA, small interference; m.o.i., multiplicity of infection; VSV, vesicular stomatitis virus; IRF, IFN regulatory factor; Ub, ubiquitin; ORF, open reading frame; RD, repressor domain.

CARD-like domains of RIG-I thereby facilitating the RIG-I-mediated activation of type I IFN signaling (23, 24), although Shimotohno and co-workers (25) previously reported that TRIM25 (EFP) does not polyubiquitinate the RIG-I CARD-like region as far under their conditions. Expression of TRIM25 increases RIG-I CARD-like region-mediated signaling; however, it remains to be determined whether the activation of full-length RIG-I requires other ubiquitin ligase (23). Another ubiquitin ligase RNF125 mediates lysine 48-linked polyubiquitination of RIG-I, which leads to degradation of RIG-I through the proteasome (25).

Here we examined what molecular complex participates in an early RIG-I-mediated RNA recognition and IFN signaling by yeast two-hybrid screening. Here we detected two novel RING finger proteins that bound to RIG-I, and we found that one, RNF135, facilitated RIG-I-mediated type I IFN induction via ubiquitinating RIG-I. RNF135 plays a crucial role in the RIG-I response to minimal copies of viral RNA, and by binding to the C-terminal helicase and RD regions of RIG-I, RNF135 facilitates RIG-I C-terminal ubiquitination to up-regulate RIG-I-mediated IFN signaling and suppress viral replication. Hence, we renamed it as RNF135 Riplet (RING finger protein leading to RIG-I activation). To our knowledge, this is the first study demonstrating that C-terminal ubiquitination of RIG-I is important for full IFN induction by RIG-I.

EXPERIMENTAL PROCEDURES

Cell Cultures—HEK293 and Vero cells were cultured in Dulbecco's modified Eagle's medium with 10% fetal calf serum (Invitrogen), and HeLa cells were in minimum Eagle's medium with 2 mM L-glutamine and 10% fetal calf serum (JRH Biosciences). HEK293FT cells were maintained in Dulbecco's modified Eagle's high glucose medium containing 10% heat-inactivated fetal calf serum (Invitrogen).

Plasmids—cDNA fragment encoding a C-terminal region of Riplet was isolated by yeast two-hybrid screening using human lung cDNA library. The 5′ region encoding the remaining N-terminal region was amplified by PCR using primers Riplet-F1 and Riplet-R1, and human lung cDNA library was used for its template. Two cDNA fragments, which cover the entire ORF of Riplet, were joined by PCR using primers Riplet-F1, R1, F2, and R2 and then inserted into pCR-blunt vector (Invitrogen). The primers sequences are as follows: F1, GCCTCGAGGCCACCATGGCGGGCCTGGGCCTGGG; R1, CGGCCAGGTCCTGCAGTAGC; F2, GCACCTGCGGAAGAACACGC; and R2, GGGGATCCCACCTTTACTTGCTTTATTATCAGG. The obtained cDNA was cloned into XhoI-NotI restriction sites of pEF-BOS expression vector, and the HA tag was fused at the C-terminal end of Riplet. Riplet-DN (dominant negative) expression vector was constructed by amplifying the relevant Riplet cDNA fragment using the primers Riplet-X-F-C and Riplet-R2 and subcloned into pEF-BOS. The primer sequence of Riplet-X-F-C was as follows: GCTCGAGGCCACCATGCCGCACCTGCGGAAGAACACGC. Riplet-L248fs expression vector was made by deleting 1 base at position 742 by standard PCR-mediated site-directed mutagenesis methods with primers Riplet-L248fs-F and Riplet-L248fs-R as follows: Riplet-L248fs-F, CCAGAGCCACCCTGCATCAGGAGAGCTTCTCGG, and Riplet-L248fs-R, CCGAGAAGCTCTCCTGATGCAGGGTGGCTCTGG. All cloned *RIPLET* cDNA fragments were sequenced, and it was confirmed that there were no mutations. Full-length RIG-I expressing vector, Gal4-IRF-3, Gal4-DBD, and p55 UASG-Luc reporter plasmids were gifts from Dr. T. Fujita (Kyoto University, Kyoto, Japan). p125 luc reporter plasmid was a gift from Dr. T. Taniguchi (University of Tokyo, Tokyo, Japan). RIG-I RD expressing vector was made with primers RIG-I RD-F and RIG-I RD-R; the RIG-I dRD cDNA fragment, which encodes ORF of RIG-I from the 1- to 754-amino acid region, was made by using primers RIG-I-(1–754)F and RIG-I-(1–754)R. The obtained cDNA fragments were sequenced, and it was confirmed that there were no mutations caused by PCR. The primers sequences are as follows: RIG-I RD-F, GAT GAT AAA GGT ACC ACC GGT AGC AAG TGC TTC CTT CTG; RIG-I RD-R, AAG GAA GCA CTT GCT ACC GGT GGT ACC TTT ATC ATC ATC ATC; RIG-I-(1–754)F, GC AGA GGA AGA GCA AGA TGA TAT CAG GTC CTC AAT CTT C; and RIG-I-(1–754)R, ATT GAG GAC CTG ATA TCA TCT TGC TCT TCC TCT GCC TC.

Northern Blotting—Human *RIPLET* 1092-bp cDNA fragment (208–1299) was used for the probe for Northern blotting. The Northern blot membranes, human 12-lane MTN blot and MTN blot III, were purchased from Clontech. The homology of human *RIPLET* and *TRIM25* in the probe region was 46%. We used a stringent condition for Northern blotting to exclude the cross-hybridization between the *RIPLET* and *TRIM25* genes. Briefly, the probe was labeled with [α-^{32}P]dCTP using Rediprime II Random Prime labeling system (GE Healthcare). The labeled probe was hybridized to the membrane with ExpressHyb hybridization solution (Clontech) at 68 °C for 1 h. The membrane was washed with washing solution I (2× SSC, 0.05% SDS) for 40 min, and then washed with washing solution II (0.1× SSC, 0.1% SDS) for 40 min. Riplet mRNA bands were detected with x-ray film.

Reporter Gene Analysis—HEK293 cells were transiently transfected in 24-well plates using FuGENE HD (Roche Applied Science) with expression vectors, reporter plasmids, and internal control plasmid coding *Renilla* luciferase. The total amounts of plasmids were normalized with empty vector. For poly(I-C) stimulation, 24 h after transfection, cells were stimulated with medium containing poly(I-C) (50 μg/ml) and DEAE-dextran (0.5 mg/ml) for 1 h, and then the medium was exchanged with normal medium and incubated for an additional 3 h. Cells were lysed with lysis buffer (Promega) and luciferase, and *Renilla* luciferase activities were measured by the dual luciferase assay kit (Promega). Relative luciferase activities were calculated by normalizing luciferase activity by *Renilla* luciferase activity, and dividing the normalized value by control in which only empty vector, reporter, and internal control plasmid were transfected. Values are expressed as mean relative stimulations ± S.D. for a representative experiment, and each was performed three times in duplicate (unless otherwise indicated in the legends).

RNA Interference—Reporter and siRNA (20 nM final concentration) for Riplet or control were transfected into HEK293 cells with Lipofectamine 2000 (Invitrogen) by the standard method described in the manufacturer's protocol. Empty vec-

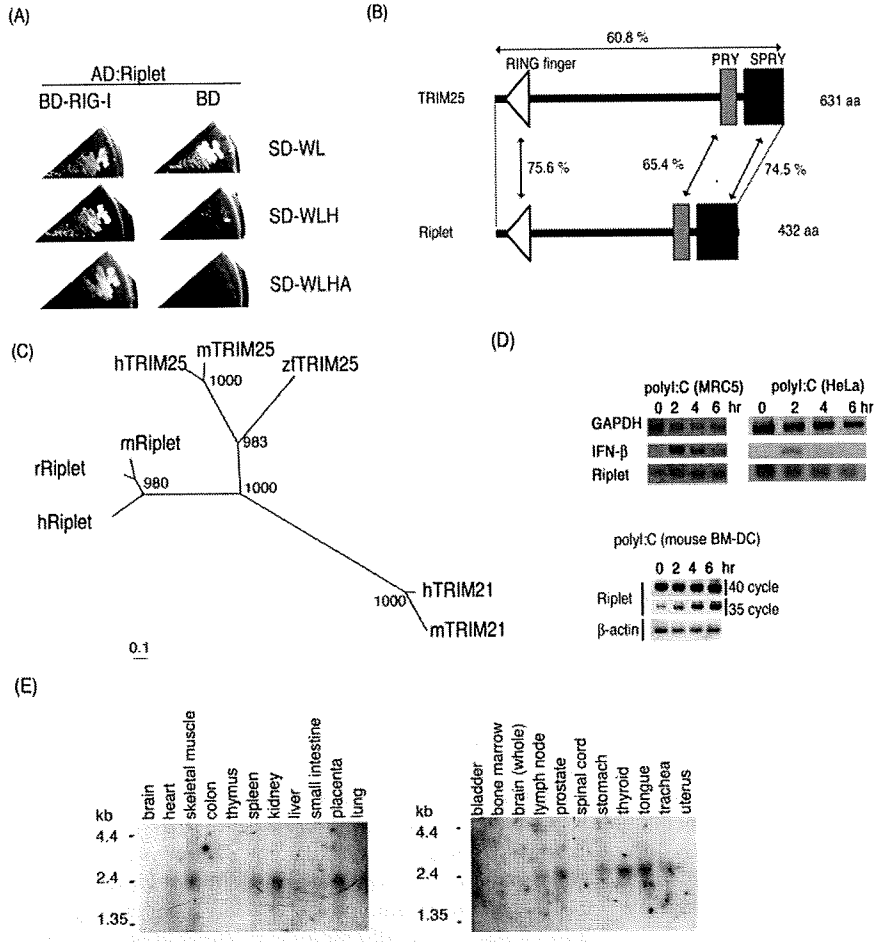

FIGURE 1. **Isolation of Riplet by yeast two-hybrid screening.** *A*, yeast cells carrying both RIG-I and Riplet can grow in selective media (SD-WLH, SD-WLHA), whereas yeast cells carrying RIG-I alone only grow in nonselective media (SD-WL), indicating the physical interaction of RIG-I with Riplet. *B*, human Riplet protein sequence is 60.8% identical to human TRIM25. The RING finger domains and SPRY motifs show higher sequence similarities between the two proteins. *aa*, amino acids. *C*, phylogenetic tree constructed by the Neighbor-Joining method shows that Riplet is similar to TRIM25. *h*, *m*, *r*, or *zf* represent human, mouse, rat, or zebrafish, respectively. The *numbers* on the node are bootstrap probabilities (n = 1000). *D*, HeLa cell, human primary-cultured fibroblast cell, MRC5, or bone marrow-derived mouse dendritic cell (*BM-DC*) were stimulated with poly(I-C) (50 μg/ml) for indicated hours. Total RNA was extracted with TRIzol reagent, and then RT-PCR was carried out using primers shown under "Experimental Procedures." *GAPDH*, glyceraldehyde-3-phosphate dehydrogenase. *E*, Northern blot membranes containing 1 μg of poly(A)$^+$ RNA per lane from human tissues were blotted with human Riplet probe.

tor was added to normalize the final plasmid amount. 48 h after transfection, cells were stimulated with poly(I-C) for 4 h. For VSV infection, 24 h after transfection, cells were infected with VSV at m.o.i. = 1, and cell lysate was prepared after 12 h for reporter gene assays. The degree of gene silencing was confirmed by RT-PCR using RNA extracted from cells 24 h after transfection. PCR primers used for the RT-PCR were Riplet-F3 (ACTGGGAAGTGGACACTAGG) and Riplet-R3 (ACTCATACAGAAGCTTCTCC). siRNAs were purchased from Funakoshi Co., Ltd. (Tokyo Japan), and the siRNA sequences of Riplet siRNA were GACUAUGGACUCUUGUUGUGU (sense) and ACAACAAGAGUCCAUAGUCCU (antisense). Control siRNA sequences were CUGUUGGUUUAGUAAGCCUGU (sense) and AGGCUUACUAAACCAACAGUC (antisense). Another siRNA, Riplet si-1, and control negative siRNA (silencer negative control 1 siRNA, AM4611) were purchased from Applied Biosystems. siRNA sequences were Riplet si-1 GGGAAAGCUUGCCUUCUAUdTdT (sense) and AUAGAAGGCAAGCUUUCCCdTdC (antisense).

Virus Preparation and Infection—VSV Indiana strain and poliovirus were amplified using Vero cells. HEK293 cells were transfected in 24-well plates with plasmid encoding *RIG-I*, Riplet, or no insert. 24 h after transfection, cells were infected with viruses for 24 h, and the titers of virus in culture supernatant were measured by plaque assay using Vero cells. For RNA interference assay, cells were transfected with siRNA with Lipofectamine 2000. 24 h after transfection, cells were infected with viruses at m.o.i. = 0.001 for 18 h, and the titer in culture supernatant were determined by plaque assay.

Immunoprecipitation—HEK293FT cells were transfected in 6-well plates with plasmids encoding FLAG-tagged RIG-I and/or HA-tagged Riplet. The plasmid amounts were normalized by the addition of empty plasmid. 24 h after transfection, cells were lysed with lysis buffer (20 mM Tris-HCl (pH 7.5), 125 mM NaCl, 1 mM EDTA, 10% glycerol, 1% Nonidet P-40, 30 mM NaF, 5 mM Na_3VO_4, 20 mM iodoacetamide, and 2 mM phenylmethylsulfonyl fluoride), and then proteins were immunoprecipitated with rabbit anti-HA polyclonal (Sigma) or anti-FLAG M2 monoclonal antibody (Sigma). The precipitated samples were analyzed by SDS-PAGE and stained with anti-HA (HA1.1) (Covance) or anti-FLAG M2 monoclonal antibody. For ubiquitination assay of RIG-I, the plasmid encoding two multiple HA-tagged ubiquitins was used. HEK293FT cells were transfected with plasmids encoding FLAG-tagged RIG-I, Riplet, or 2× HA-tagged ubiquitin. 24 h after transfection, cells were lysed, and then RIG-I was immunoprecipitated as described above. The samples were analyzed by SDS-PAGE and stained with anti-HA polyclonal antibody (for detection of ubiquitination) or anti-FLAG monoclonal antibody (for detection of RIG-I). Reproducibility was confirmed with additional experiments (see supplemental figures).

Construction of RIG-I 3KA and 5KA Mutant Genes—The C-terminal three or five lysine residues were mutated into alanines (designated as 3KA and 5KA). RIG-I 3KA has K888A, K907A, and K909A, whereas RIG-I 5KA has K849A, K851A,

K888A, K907A, and K909A. The mutant *rig-I* genes were made by PCR-mediated site-directed mutagenesis. The primers used for the PCR were as follows: K907–909A-forward, GTT CAG ACA CTG TAC TCG GCG TGG GCG GAC TTT CAT TTT GAG AAG, and K907–909A-reverse, CTT CTC AAA ATG AAA GTC CGC CCA CGC CGA GTA CAG TGT CTG AAC; K888A-forward, GAC ATT TGA GAT TCC AGT TAT AGC AAT TGA AAG TTT TGT GGT GGA GG, and K888A-reverse, CCT CCA CCA CAA AAC TTT CAA TTG CTA TAA CTG GAA TCT CAA ATG TC; K849–851A-forward, GAG TAG ACC ACA TCC CGC CCA GCG CAG TTT TCA AGT TTT G, and K849–851A-reverse, CAA AAC TTG AAA ACT GCG CTG GCG CGG GAT GTG GTC TAC TC. PCR was carried with Pyrobest *Taq* polymerase, and the obtained clones were sequenced to exclude the clones harboring PCR error. To construct the plasmid-expressing mutant RIG-I protein, the wild-type *RIG-I* gene on pEF-BOS vector was replaced with the mutant *rig-I* gene.

Real Time PCR—Quantitative PCR analyses were carried out using iCycler iQ real time detection system with Platinum SYBR Green qPCR SuperMix-UDG reagent (Invitrogen). Primer sequences for qPCR were as follows: hGAPDH-qF, GAG TCA ACG GAT TTG GTC GT, and hGAPDH-qR, TTG ATT TTG GAG GGA TCT CG; hIFN-β-qF, TGG GAG GAT TCT GCA TTA CC, and hIFN-β-qR, CAG CAT CTG CTG GTT GAA GA; hMx1-qF, ACC ACA GAG GCT CTC AGC AT, and hMx1-qR, CTC AGC TGG TCC TGG ATC TC; and hIFIT-1-qF, GCA GCC AAG TTT TAC CGA AG, and hIFIT-1-qR, CAC CTC AAA TGT GGG CTT TT. Values were expressed as mean relative stimulations, and for a representative experiment from a minimum of three separate experiments, each was performed in triplicate.

RESULTS

RIG-I-binding Proteins—To isolate the proteins that bind to RIG-I, we performed yeast two-hybrid screening using a human lung cDNA library. Using the RIG-I central region (213–601 amino acids), we isolated a clone that encoded a partial ORF of a gene expressed in a dendritic cell line, DC12, whereas the C-terminal region of RIG-I (557–925 amino acids) resulted in the isolation of two cDNA clones, which encoded partial C-terminal regions of ZNF598 and RNF135 (Fig. 1*A* and data not shown). Preliminary expression studies showed that the RNF135 segment affected the RIG-I IFN-β inducing activity, whereas the other two proteins had no effect (data not shown). We confirmed the

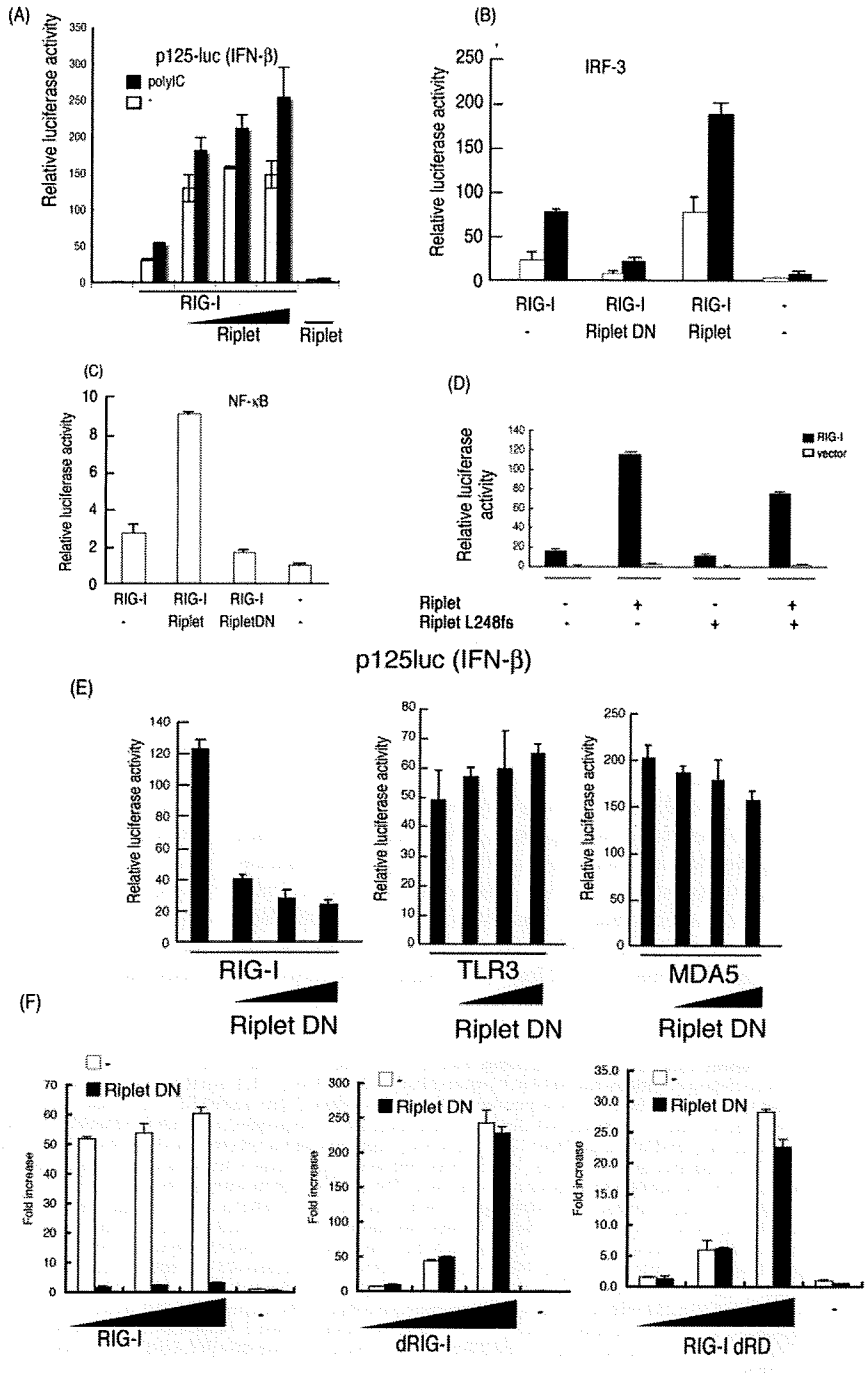

interaction of RIG-I with ZNF598 or RNF135 in HEK293FT cells by immunoprecipitation (data not shown). RNF135 was previously annotated by the genome project and was recently found to be a cause of a genetic disease, neurofibromatosis, although its protein function was unknown. We renamed the protein Riplet (RING finger protein leading to RIG-I activation) based on the following functional analyses. Riplet was most similar to TRIM25 (60.8% sequence homology), in particular between their RING finger domains PRY or SPRY (Fig. 1*B*). Phylogenetic analysis also supported the notion that Riplet was similar to TRIM25 (Fig. 1*C*). Thus, we hypothesized that, like TRIM25, Riplet is a ubiquitin ligase.

Expression of Riplet—RIG-I mRNA is induced by type I IFN or poly(I-C) stimulation in mammalian cells. Unlike RIG-I, however, Riplet mRNA was basally expressed in HeLa and primary-cultured MRC-5 cells irrespective of stimulation (Fig. 1*D* and data not shown). On the other hand, when we treated bone marrow-derived dendritic cells with poly(I-C), the basal level of Riplet mRNA was increased by the stimulation (Fig. 1*D*), suggesting that the regulatory mechanism of Riplet expression somewhat differs among cell types, and that Riplet is expressed before virus infection in some cell types. Next we performed Northern blotting of human tissue RNA. Riplet mRNA was detected as a single band of 2.4 kbp, which is slightly longer than the RNF135 cDNA sequence deposited in GenBank™ (accession number AB470605). Human *RIPLET* is expressed in human skeletal muscle, spleen, kidney, placenta, prostate, stomach, thyroid, and tongue and also weakly expressed in heart thymus, liver, and lung (Fig. 1*E*).

Riplet Enhances RIG-I-mediated IFN-β Induction—At first we characterized the role of Riplet in RIG-I-mediated IFN inducing signaling by reporter gene analyses. When RIG-I was expressed in HEK293 cells, reporter auto-activation was observed even in the absence of exogenous stimulation (Fig. 2*A*) as reported previously (25, 26). Stimulation with poly(I-C) further enhanced the promoter. Co-expression of Riplet with RIG-I potentiated activation of the IFN-β promoter, whereas expression of Riplet alone resulted in only marginal activation (Fig. 2*A*). Detection of endogenous IFN-β mRNA confirmed that Riplet enhanced RIG-I-mediated activation of IFN-β transcription (supplemental Fig. S1). The enhancing role of Riplet in IFN-β promoter activation was also supported by activation of IRF-3 and NF-κB by Riplet (Fig. 2, *B* and *C*). In contrast, expression of a Riplet partial fragment (Riplet-DN) (70–432 amino acids) that lacked the N-terminal RING finger domain reduced promoter activation (Fig. 2*E*). The Riplet-L249fs mutant protein, which was isolated from neurofibromatosis patients (27), did not increase the RIG-I-mediated promoter activation (Fig. 2*D*). These data indicate that Riplet augments RIG-I-mediated IFN-β promoter activation, and that both the RING finger domain and the C-terminal region encoding the SPRY and PRY motifs are important for its function. Riplet (residues 70–432) acted as a dominant-negative form (hereafter called Riplet-DN) (Fig. 2, *E* and *F, left panel*). This functional feature of Riplet-DN was confirmed in Fig. 2, *B* and *C*, and was later confirmed through RIG-I co-precipitation and ubiquitination analyses (see Fig. 5*C* and supplemental Fig. S4*C*). Expression of Riplet-DN did not reduce TLR3 or MDA5 signaling (Fig. 2*E*), suggesting that Riplet-DN is specific for RIG-I signaling. Interestingly, the Riplet-DN only partially suppressed the function of the C-terminal deleted RIG-I (dRD), which is a constitutively active form (Fig. 2*F, right panel*), and RIG-I CARD-like region (dRIG-I)-mediated signaling in high or low dose transfection of dRIG-I was barely inhibited by overexpression of Riplet-DN (Fig. 2*F, center panel*). These data suggest that Riplet requires the RIG-I C-terminal domain (RD) and partial helicase region to activate RIG-I signaling.

Endogenous Riplet Promotes the RIG-I Signaling—We performed Riplet knockdown by siRNA Riplet using Lipofectamine 2000 reagents, instead of FuGENE HD, to reveal the function of endogenous Riplet. Two siRNAs (Riplet siRNA and Riplet si-1) that target different sites of the Riplet mRNA and two control siRNAs were used for knockdown analyses. The two siRNA or control siRNA were co-transfected with HA-tagged Riplet expression vector into HEK293 cells, and after 48 h, cell lysate was prepared and analyzed by Western blotting with anti-HA antibody detecting Riplet. The two siRNAs targeting Riplet abolished exogenously expressed Ripelt-HA, but control siRNA did not (supplemental Fig. S3). Likewise, both Riplet siRNA and Riplet si-1 specifically down-regulate the level of endogenous Riplet mRNA (Fig. 3, *A* and *B*).

Using the siRNA, we examined whether Riplet knockdown reduces RIG-I signaling. As expected, RIG-I-mediated IFN-β promoter activation was reduced by Riplet siRNA or Riplet si-1 compared with control siRNA (Fig. 3, *A* and *B*), indicating that Riplet is required for full activation of the RIG-I signaling. Vesicular stomatitis virus (VSV) is a negative-stranded RNA virus that induces IFN-β production via RIG-I (3). Although the

FIGURE 2. **Riplet enhances IFN-β signaling mediated by RIG-I.** *A*, Riplet enhances the promoter activation by RIG-I. HEK293 cells were transfected with plasmids encoding empty vector, RIG-I (0.1 μg) and Riplet (0.025, 0.05, or 0.1 μg) together with p125-luc (IFN-β promoter) reporter plasmid in 24-well plates. 24 h after transfection, the cells were treated with mock or poly(I-C) (50 μg/ml) for 4 h as described under "Experimental Procedures," and then luciferase activities of cell lysates were measured. *Closed* or *open boxes* represent poly(I-C) or mock stimulation, respectively. *B*, to examine the activation of IRF-3, RIG-I (0.1 μg), Riplet (0.1 μg), and/or Riplet-DN (0.1 μg),expressing vectors were transfected into HEK293 cells with reporter plasmids, GAL4 fused IRF-3 (0.05 μg), and the p55 UASG-luc reporter gene (0.05 μg), in which luciferase reporter gene is fused downstream of GAL4 protein-binding site, and therefore activated IRF-3 promotes the transcription of luciferase reporter gene. The cells were stimulated with poly(I-C) as described above (34). The total amount of transfected DNA (0.5 μg/well) was kept constant by adding empty vector (pEF-BOS). *C*, HEK293 cells were transfected with RIG-I (0.1 μg), Riplet (0.1 μg), and/or Riplet-DN (0.1 μg) expressing vectors together with the NF-κB reporter plasmid (0.1 μg), and 24 h later, the luciferase activities of cell lysates were measured. *D*, Riplet-L248fs, which lacks the C-terminal region, did not enhance the activation at all. HEK293 cells were transfected with the plasmids expressing wild-type Riplet (0.1 μg) or Riplet-L248fs (0.1 μg) together with RIG-I expressing vector (0.1 μg) and p125-luc reporter (0.1 μg). 24 h after transfection, cell were stimulated with poly(I-C), and the luciferase activities of cell lysates were determined as described above. *E*, RIG-I (0.1 μg), MDA5 (0.1 μg), or TLR3 (0.1 μg) expressing vectors were transfected into HEK293 cells with the plasmid encoding the Riplet-DN fragment (0.1, 0.2, or 0.3 μg) in 24-well plates. After 24 h, the cells were stimulated with 50 μg of poly(I-C) for 4 h, and relative luciferase activities were determined. *F*, Riplet-DN (100 ng) was co-transfected with full-length RIG-I (0, 50, 100, or 200 ng), RIG-I CARD-like region (dRIG-I) (0, 50, 100, or 200 ng), or C-terminal deleted RIG-I (RIG-I dRD) (0, 50, 100, or 200 ng) into HEK293 cells in 24-well plate, and reporter gene assays were carried out.

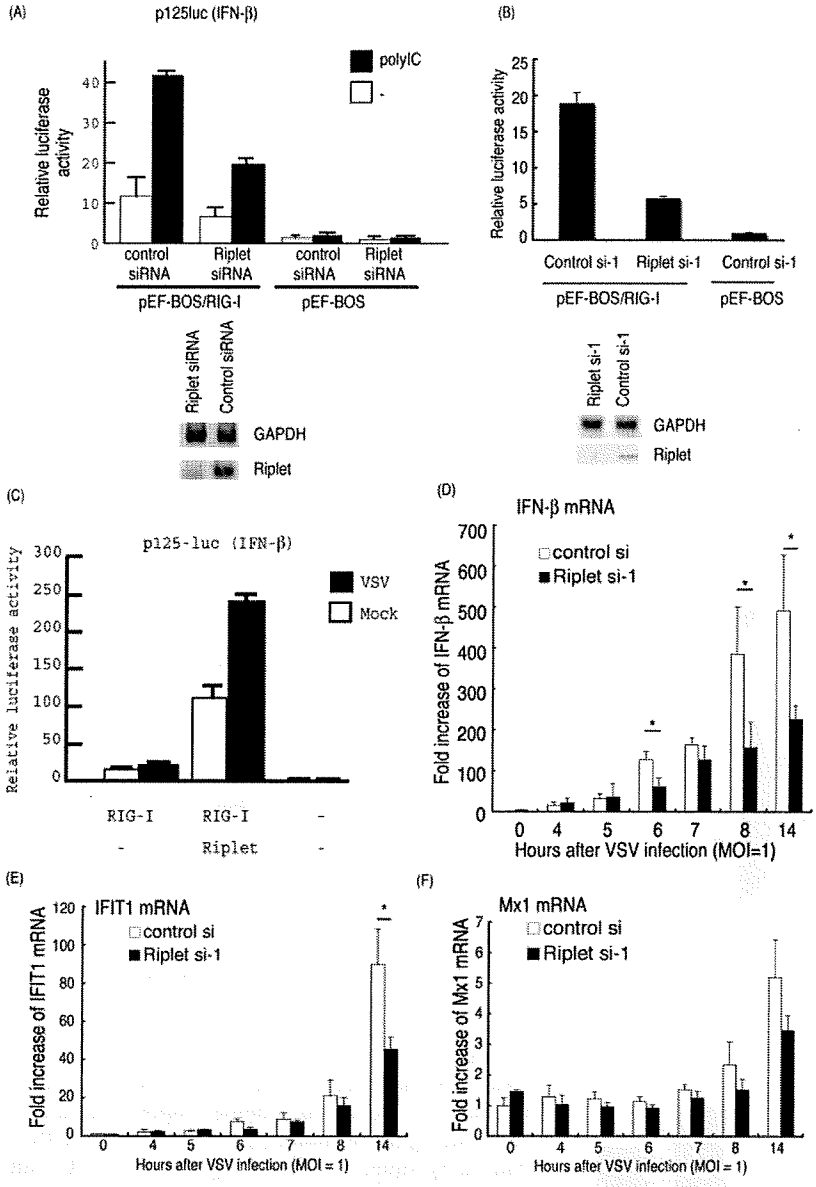

FIGURE 3. **Knockdown analyses of Riplet.** *A*, p125 luc reporter plasmid (0.1 μg), RIG-I expressing vector (0.1 μg), and Riplet siRNA or control siRNA (10 pmol), which were purchased from Funakoshi Co. Ltd., were transfected into HEK293 cells in a 24-well plate with Lipofectamine 2000, and 48 h after transfection, the cells were stimulated with poly(I-C) for 6 h, and the cell lysate was prepared, and luciferase activities were measured. RT-PCR was carried out using total RNA extracted from cells 48 h after transfection. *B*, p125 luc reporter plasmid (0.1 μg), RIG-I expressing vector (0.1 μg), and siRNA, Riplet si-1, or control si-1 (10 pmol), which were purchased from Applied Biosystems, were transfected into HEK293 cells with Lipofectamine 2000. 48 h after transfection, the cells were stimulated with poly(I-C) for 6 h. The cell lysate was prepared, and luciferase activities were measured. RT-PCR was carried out using total RNA extracted from cells 48 h after transfection. *C*, HEK293 cells were transfected with the plasmids expressing RIG-I (0.1 μg) and/or Riplet (0.1 μg) with p125 luc reporter plasmid (0.1 μg) in 24-well plates. After 24 h, the cells were infected with VSV (m.o.i. = 1) for 12 h. The luciferase activities of the cell lysates were measured. Expression of Riplet strongly enhanced IFN-β promoter activation by VSV through RIG-I. *D–F*, siRNA (control si- or Riplet si-1) were transfected into HEK293 cells, and after 48 h, the cells were infected with VSV at m.o.i. = 1. RNA was extracted at the indicated hours, and the quantitative PCR were carried out to detect the expression of IFN-β (*D*), IFIT-1 (*E*), or Mx1 (*F*) mRNA. *, $p < 0.05$. *GAPDH*, glyceraldehyde-3-phosphate dehydrogenase.

IFN-β promoter was only minimally activated by RIG-I in response to VSV (m.o.i. = 1) during the early phase of infection (<12 h), the activity was increased by RIG-I and Riplet (Fig. 3*C*). Riplet was silenced by siRNA and then VSV infected the cells. VSV-derived up-regulation of IFN-β mRNA was started around 6 h post-infection, and Riplet siRNA significantly suppressed the increase of IFN-β mRNA at 6 h (Fig. 3*D*). Because VSV infection is mainly sensed by RIG-I, this is consistent with the notion that Riplet promotes the RIG-I signaling. Other IFN-inducible genes, *IFIT1* and *MX1*, were expressed >8 h post-infection, and their expressions were also suppressed by Riplet siRNA (Fig. 3, *E* and *F*).

Riplet Exerts Protective Activity against Viral Infection—Next we examined the role of Riplet during viral infection. Riplet and/or RIG-I were transiently expressed in the human cells by FuGENE HD reagents, and then the cells were infected with VSV or poliovirus (a positive-stranded RNA virus). The viral titer of the supernatant was determined 24 h post-infection. Under our conditions, expression of RIG-I weakly inhibited VSV propagation. Co-expression of Riplet with RIG-I significantly suppressed VSV replication especially at low m.o.i., whereas Riplet alone did not suppress VSV (Fig. 4, *A* and *B, upper panel*). Therefore, a sufficient amount of RIG-I protein is required for Riplet to exert antivirus activity. This requirement of RIG-I is also observed in reporter gene analyses (Fig. 2). Under a similar setting, the antiviral effect of Riplet was marginally observed against poliovirus, which induces IFN-β largely via MDA5 (Fig. 4*B*, *lower panel*). To assess the importance of endogenous Riplet for antivirus effect of human cells, Riplet knockdown cells were infected with viruses. In Riplet knockdown cells, the VSV titer was consistently increased compared with the control ($p < 0.05$) (Fig. 4*C*, *left panel*). In addition, infection of Riplet knockdown cells with poliovirus resulted in only a slight increase in the poliovirus titer compared with the control ($p > 0.05$) (Fig. 4*C*, *right panel*). Because poliovirus is mainly recognized by MDA5 but not RIG-I, this marginal effect of Riplet on poliovirus infection was within expectation (3, 28).

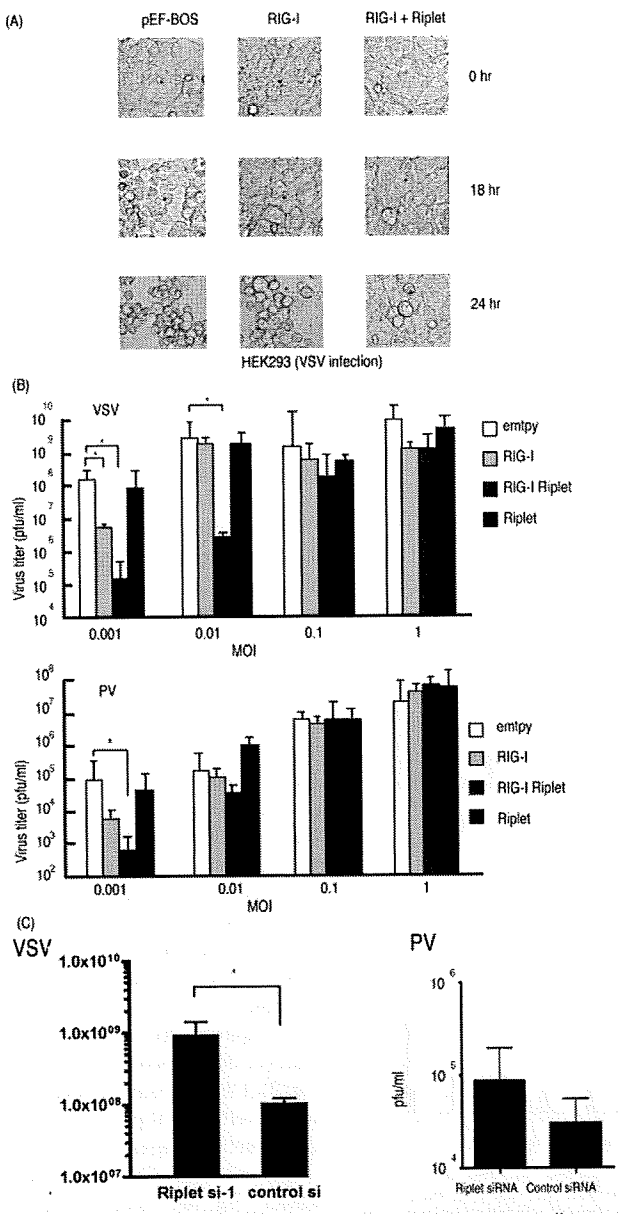

FIGURE 4. **Suppression of RNA viruses by Riplet.** *A*, HEK293 cells were transfected with RIG-I (0.1 μg) and/or Riplet (0.1 μg) expressing vectors. The total amount of transfected DNA (0.5 μg/well) in each well was kept constant by adding empty vector (pEF-BOS). 24 h after transfection, the cells were infected with VSV at m.o.i. = 0.1, and after 0, 18, or 24 h, CPE was observed by microscope. *B*, RIG-I (0.1 μg) and/or Riplet (0.1 μg) expressing plasmids were transfected to HEK293 cells in 24-well plates and incubated for 24 h. The total amount of transfected DNA (0.5 μg/well) in each well was kept constant by adding empty vector (pEF-BOS). The cells were infected with VSV (*upper panel*) or poliovirus (*PV*) (*lower panel*) at the indicated m.o.i. The viral titers in the culture media were measured 24 h after infection by plaque assay. *Error bars* represent standard deviation ($n = 3$). *, $p < 0.05$. *C*, control or Riplet knockdown HEK293 cells were infected with VSV (*left panel*) or poliovirus (*right panel*) at m.o.i. = 0.1. The viral titers in the culture media were measured 26 h after infection by plaque assays. Knockdown of Riplet induced higher VSV titers compared with control ($p < 0.05$), but the increase observed in poliovirus-infected Riplet knockdown cells was not significant ($p > 0.05$).

Riplet and Riplet-DN Bind the Helicase and RD Regions of RIG-I—Yeast two-hybrid analysis showed that a C-terminal region of Riplet bound to the C-terminal region of RIG-I. This cytoplasmic interaction between Riplet and RIG-I was confirmed by confocal microscopy in HeLa cells (supplemental Fig. S2). To further confirm the physical binding of Riplet to RIG-I in human cells, we carried out immunoprecipitation analyses. Full-length Riplet was co-immunoprecipitated with RIG-I (Fig. 5*B*), indicating that Riplet binds directly to RIG-I in human cells.

To determine the region responsible for the RIG-I-Riplet interaction, we constructed a RIG-I and Riplet deletion series as shown in Fig. 5*A*. Riplet-DN also bound to RIG-I (Fig. 5, *B* and *C*), indicating that the RING finger domain is dispensable for the RIG-I-Riplet interaction. This is consistent with the notion that the RING finger domain in ubiquitin ligase proteins is required for their interactions with ubiquitin-conjugating enzymes (29). Unlike TRIM25, Riplet and Riplet-DN failed to co-precipitate the two CARD domains of RIG-I (dRIG-I) (Fig. 5*D*). However, co-precipitation of the RIG-IC or RIG-RD fragments was observed (Fig. 5, *E* and *F*). RD-deleted RIG-I (RIG-I dRD) weakly associated with Riplet (Fig. 5*G*). Taken together, Riplet preferentially binds the RD and also weakly associates with the helicase region of RIG-I with its C terminus. Reporter gene analyses show that Riplet-DN only weakly suppresses RIG-I signaling and barely suppresses dRIG-I, which contains neither helicase nor RD region. Therefore, the physical interaction is correlated with the results of reporter activity.

Riplet Promotes Ubiquitination of RIG-I—Because Riplet shares 60% sequence similarity with TRIM25, we hypothesized that Riplet ubiquitinates RIG-I and that this modification leads to activation of RIG-I signaling. To test this hypothesis, we examined RIG-I ubiquitination. As expected, ubiquitination of RIG-I was increased by co-expression of Riplet under two different conditions (Fig. 6, *A* and *B*). The quantity of RIG-I ubiquitination was significantly high in the presence of Riplet (Fig. 6*C*). RIG-I ubiquitination was suppressed if Riplet was replaced with Riplet-DN (Fig. 6*D* and supplemental Fig. S4*C*). However, unlike TRIM25, Riplet binds to the C-terminal region of RIG-I. Therefore, we examined whether Riplet ubiquitinates the C-terminal region. We found that ubiquitination of RIG-IC was enhanced by Riplet expression (Fig. 6*E*). Both RIG-I dRD and RIG-I RD were also ubiquitinated by expression of Riplet (Fig. 6*F*; supplemental Fig. S4*A* and S5), suggesting that Riplet promotes ubiquitination of the helicase and RD domains of RIG-I in a manner distinct from TRIM25.

Ubiquitin is polymerized through its lysine residue. Lys-63-linked polyubiquitination is frequently observed in signal transduction pathways (30). In contrast, Lys-48-linked polyubiquitination usually leads to the degradation of protein through the proteasome. Indeed, TRIM25-mediated Lys-63-linked polyubiquitination activates the CARD-like region of RIG-I, and RNF125-mediated Lys-48-linked polyubiquitination leads to the degradation of RIG-I (23, 25). We used K48R or K63R mutated ubiquitin and found that K48R was incorporated normally into RIG-IC, whereas polyubiquitination was decreased by K63R (supplemental Fig. S4*B*). K63R mutation abolished RIG-I RD polyubiquitination by Riplet (Fig. 6*F*). These data

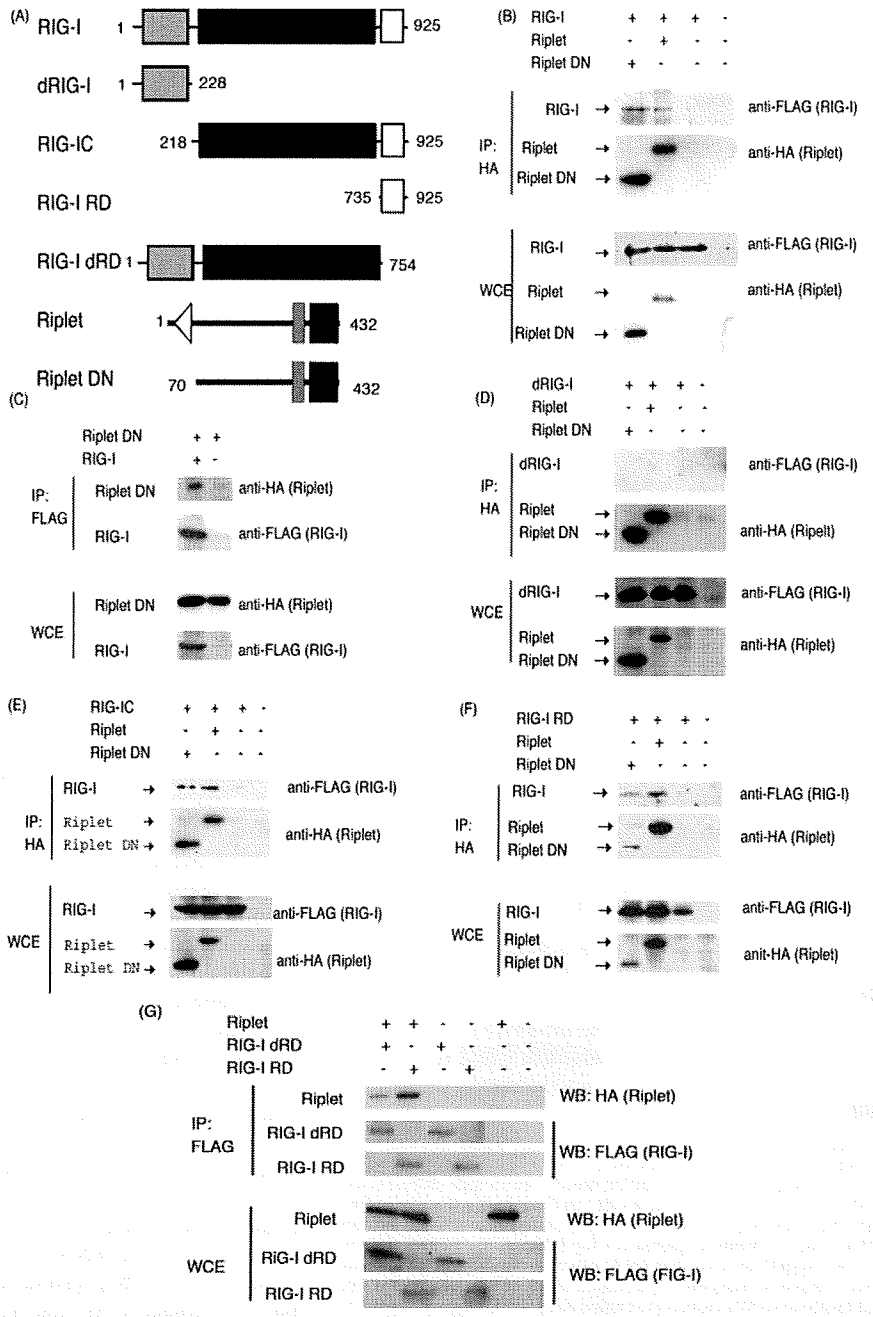

FIGURE 5. **Physical interaction of Riplet with RIG-I.** *A*, schematic representation of RIG-I or Riplet fragments used for immunoprecipitation analyses. *B*, HA-tagged Riplet (0.4 μg) or Riplet-DN (0.4 μg) were transfected into HEK293FT cells in a 6-well plate with FLAG-tagged RIG-I (0.4 μg). HA-tagged Riplet or Riplet-DN were immunoprecipitated (*IP*) with anti-HA antibodies, and samples were analyzed by Western blotting (*WB*) using an anti-FLAG or anti-HA antibody. The total amount of transfected DNA (2 μg/well) was kept constant by adding empty vector (pEF-BOS). *C*, HA-tagged Riplet-DN (0.4 μg) and FLAG-tagged RIG-I (0.4 μg) were transfected into HEK293FT cells in a 6-well plate. RIG-I was immunoprecipitated with anti-FLAG antibody, and samples were analyzed by Western blotting using an anti-FLAG or -HA antibody. The total amount of transfected DNA (2 μg/well) was kept constant by adding empty vector (pEF-BOS). *D–F*, interaction of HA-tagged Riplet or Riplet-DN with FLAG-tagged dRIG-I (*D*), RIG-IC (*E*), or RIG-I RD (*F*) was examined using immunoprecipitation assays. The proteins were expressed in HEK293FT cells, and HA-tagged Riplet was immunoprecipitated with anti-HA antibody, and samples were analyzed by Western blotting using an anti-FLAG or -HA antibody. *G*, FLAG-tagged RIG-I RD (0.4 μg) or RIG-I dRD (0.4 μg) was transfected with HA-tagged Riplet (0.4 μg) into HEK293 FT cells in a 6-well plate, and 24 h after transfection, immunoprecipitation was performed with anti-FLAG antibody and analyzed by Western blotting. The total amount of transfected DNA (2 μg/well) was kept constant by adding empty vector (pEF-BOS). *WCE*, whole cell extract.

indicates that Riplet mediates Lys-63-linked polyubiquitination of the RIG-I C-terminal helicase and RD region. Because Riplet-DN reduced the RIG-I-mediated signaling, we examined whether Riplet-DN reduced the RIG-I ubiquitination. As expected, Riplet-DN reduced RIG-I ubiquitination (Fig. 6*D* and supplemental Fig. S4*C*). These ubiquitination assay data are consistent with the notion that Riplet-mediated Lys-63-linked polyubiquitination of RIG-I is required for full activation of RIG-I signaling.

We tried to determine the ubiquitination sites of RIG-I using Lys-to-Ala (KA)-converting mutants. RIG-I has 25 Lys residues in its C-terminal region. These Lys residues of RIG-I were in turn mutated to Ala, and the degree of ubiquitination and IFN-β-inducing activity were determined with each mutant. RIG-I-mediated IFN-β promoter activation was normally augmented by co-expression of Riplet and 3KA RIG-I. Co-expression of Riplet and 5KA, however, and the ubiquitination level of RIG-I and IFN-β-inducing activity were simultaneously decreased (Fig. 7, *A* and *C*). Riplet-dependent augmentation of IFN-β promoter activation was largely suppressed when RIG-I was replaced with 5KA RIG-I (Fig. 7*B*). Therefore, Lys-849 and Lys-851 of RIG-I were crucial for RIG-I ubiquitination by Riplet. The results confirmed the importance of ubiquitination of specific Lys residues in the C-terminal region of RIG-I and for RIG-I-mediated IFN-β induction.

DISCUSSION

RIG-I plays a central role in the recognition of cytoplasmic viral RNA and is regulated by modification by small modifier ubiquitin or ubiquitin-like protein, ISG15. TRIM25 mediates Lys-63-linked polyubiquitination, which is essential for RIG-I activation (23), and RNF125 mediates Lys-48-linked polyubiquitination (25). RIG-I also harbors ISG15 modification, although the role of ISG15 modification *in vivo* remains to be deter-

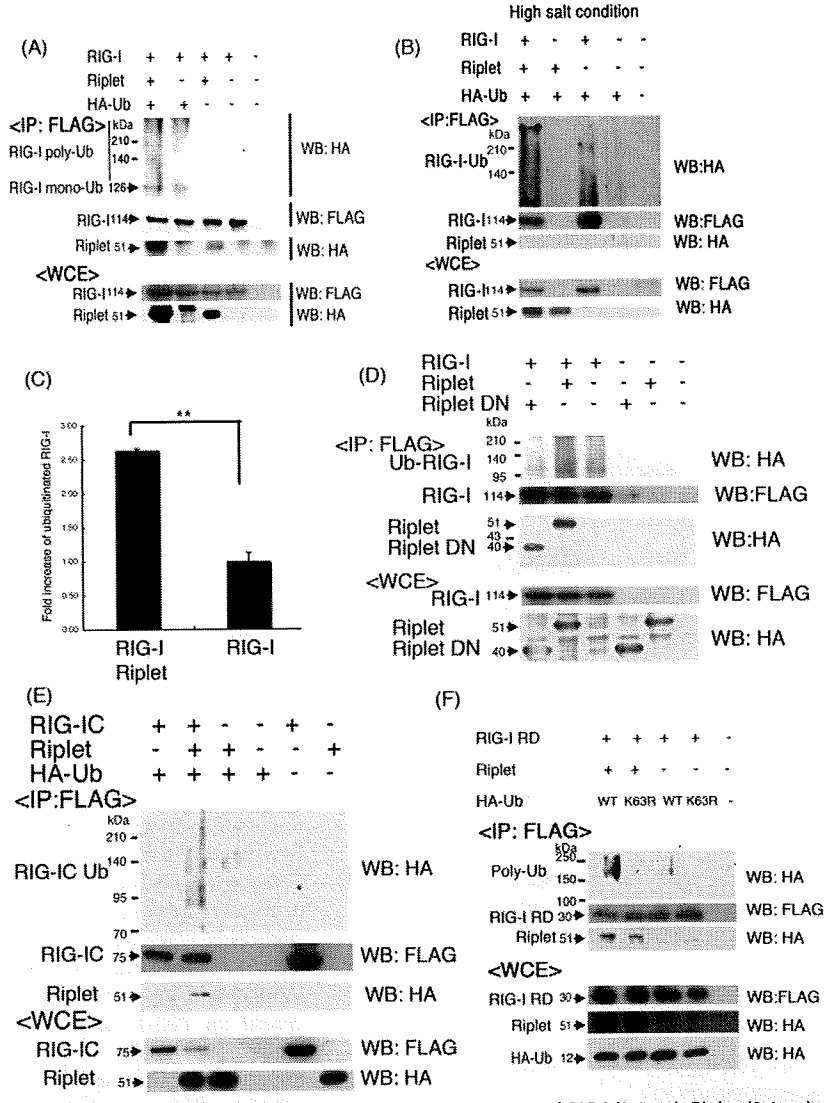

FIGURE 6. **Ubiquitination of RIG-I by Riplet.** *A* and *B*, FLAG-tagged RIG-I (0.4 μg), Riplet (0.4 μg), and HA-tagged ubiquitin (0.4 μg) expressing vectors were transfected into HEK293FT cells in 6-well plates. The total amount of transfected DNA (2 μg/well) was kept constant by adding empty vector (pEF-BOS). FLAG-tagged RIG-I was immunoprecipitated (*IP*) using an anti-FLAG antibody, and washed with the buffer containing 150 mM NaCl (*A*) or 1 M NaCl (*B*). The immunoprecipitates were separated with 8% acrylamide gel and analyzed by Western blotting (*WB*) using antibodies against HA tag (ubiquitin) or FLAG (RIG-I). Riplet was co-immunoprecipitated with FLAG-tagged RIG-I in *A* but could not co-immunoprecipitate in *B* because of high salt condition. Expression of Riplet enhanced the ubiquitination of RIG-I. Different gel conditions were employed in *A* and *B*. *C*, ubiquitinated RIG-I was quantitated with NIH image software. **, $p < 0.01$. *D*, FLAG-tagged RIG-I (0.4 μg) was transfected into HEK293 FT cells in a 6-well plate with HA-tagged Riplet (0.4 μg) or Riplet-DN (0.4 μg) and HA-tagged ubiquitin, and immunoprecipitation was carried out with anti-FLAG antibody. The total amount of transfected DNA (2 μg/well) was kept constant by adding empty vector (pEF-BOS). The samples were analyzed with 10% acrylamide gel to clearly separate Riplet from Riplet-DN and stained by Western blotting. *E*, ubiquitination of RIG-IC was also promoted by Riplet expression. HEK293FT cells were transfected with the plasmids encoding RIG-IC (0.4 μg), Riplet (0.4 μg), and/or HA-tagged ubiquitin (0.4 μg) in a 6-well plate, and 24 h after transfection, cell lysates were prepared. The total amount of transfected DNA (2 μg/well) was kept constant by adding empty vector (pEF-BOS). FLAG-tagged RIG-ICs were immunoprecipitated with anti-FLAG antibodies, and the proteins were analyzed by Western blotting. *F*, Ub-K63R are HA-tagged ubiquitin in which the lysine 3 residues were substituted with arginine. The HA-tagged Ub-K63 expressing vectors (1.2 μg), FLAG-tagged RIG-IC (0.4 μg), and/or Riplet (0.4 μg) were transfected into HEK293FT cells in 6-well plates and analyzed as shown in *A–D*. The total amount of transfected DNA (2 μg/well) was kept constant by adding empty vector (pEF-BOS). Ub-K63R was not incorporated into polyubiquitin chain of RIG-I RD. *WCE*, whole cell extract.

mined (21, 22, 31). Although Riplet and TRIM25 share 60% sequence similarity, the ubiquitination of RIG-I by Riplet is distinct from that by TRIM25; Riplet ubiquitinates the C-terminal region of RIG-I, whereas TRIM25 ubiquitinates its CARD-like region. These findings are also supported by the fact that neither Riplet nor Riplet-DN promoted or inhibited the activation of the IFN-β promoter by expression of the RIG-I CARD-like region (data not shown). It has been reported that ubiquitination of the CARD-like region of RIG-I by TRIM25 is critical for RIG-I-IPS-1 signaling (23). However, how this CARD ubiquitination is essential for activation of IPS-1 by RIG-I remains undetermined. Here we emphasize the importance of RIG-I C-terminal ubiquitination for IFN-β induction and the antiviral response. Because the C-terminal RD region inhibits the IFN inducing activity of the CARD-like region of RIG-I, it is reasonable that RIG-I C-terminal ubiquitination by Riplet inhibits the conversion from the active to inactive form of RIG-I protein after binding to viral RNA. This initial stabilization of RIG-I via ubiquitination by Riplet would provide a sufficient structure for RIG-I to maintain the accessibility to TRIM25 and facilitate TRIM25-mediated ubiquitination of the CARD-like region of RIG-I, which may lead to potential activation of IPS-1.

RIG-I is an IFN-inducible RNA helicase that is expressed at extremely low levels in resting cells (6). Initial penetration of viruses allows generation of 5′-triphosphate RNA and/or double strand RNA followed by induction of IFN-β production. This early response to viral infections triggers up-regulation of RIG-I/MDA5 and TLR3, leading to robust IFN-β production (3, 32, 33). We favor the interpretation of our present findings that during the early stages of viral infection with trace amounts of RIG-I and viral RNAs, Riplet helps host cells rearrange RIG-I conformation to activate IPS-1. This issue will need further proof because it is difficult to

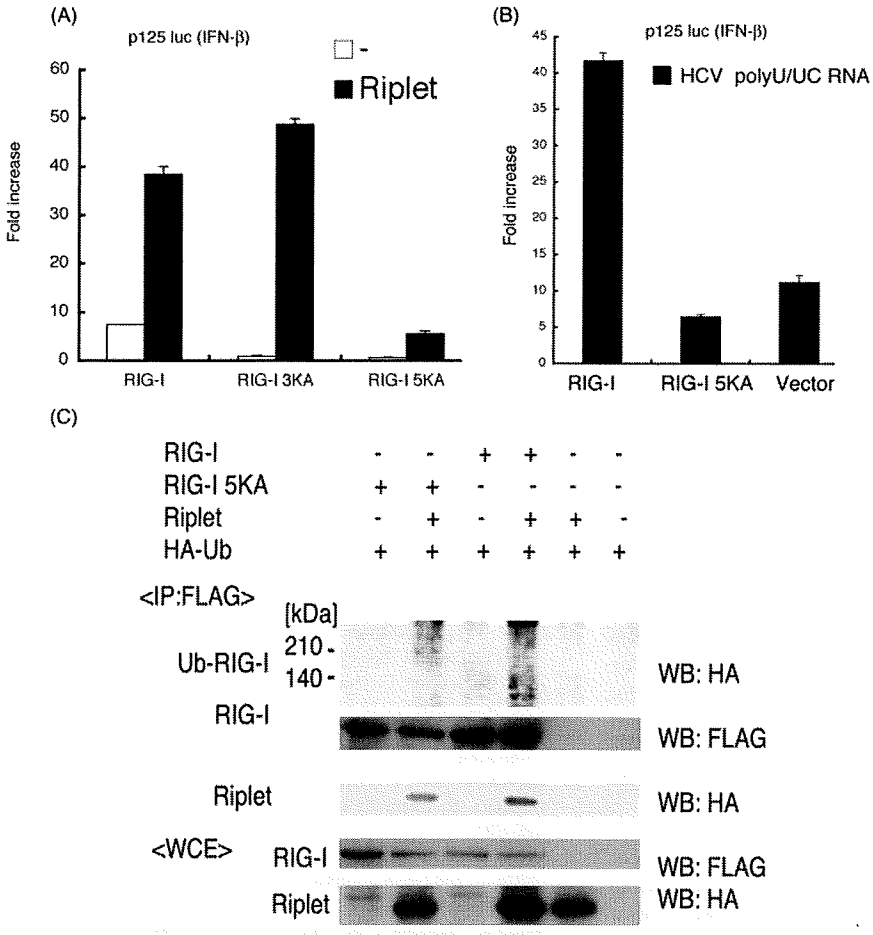

FIGURE 7. **The C-terminal two lysine residues of RIG-I are important for ubiquitination by Riplet.** *A*, RIG-I C-terminal lysine residues were substituted with alanine. RIG-I 3KA mutant protein harbors the triple mutations, K888A, K907A, and K909A. The five lysine residues, Lys-849, Lys-851, Lys-888, Lys-907, and Lys-909, were replaced with alanine in RIG-I 5KA mutant. The plasmid carrying wild-type (100 ng/well), RIG-I 3KA (100 ng/well), RIG-I 5KA (100 ng), or Riplet (100 ng) were transfected into HEK293 cells in a 24-well plate together with p125 luc reporter plasmid (100 ng/well). The amount of transfected DNA was kept constant by adding empty vector. After 24 h, the luciferase activities were measured. *B*, wild-type RIG-I (100 ng), RIG-I 5KA mutant (100 ng), or empty vector (100 ng) was transfected into HEK293 cells in a 24-well plate together with p125 luc reporter plasmids and HCV 3′-untranslated region poly(U/UC) RNA (25 ng), which is synthesized in *in vitro* transcription by T7 RNA polymerase. The amount of transfected DNA was kept constant by adding empty vector. 24 h after transfection, luciferase activities were measured. RIG-I 5KA mutant hardly responded to poly(U/UC) RNA. *C*, to observe the ubiquitinated RIG-I more clearly, we used 800 ng/well of Riplet and HA-Ub expression vector for the following transfection. HEK293FT cells in a 6-well plate were transfected with the plasmids encoding RIG-I (400 ng/well), RIG-I 5KA (400 ng/well), Riplet (800 ng/well), and/or HA-Ub (800 ng/well). The total amount of DNA was kept constant by adding the empty vector. 24 h after the transfection, the cell lysates were prepared, and the immunoprecipitation was carried out using anti-FLAG antibodies. The immunoprecipitates were analyzed by Western blotting with anti-HA or FLAG antibodies.

visualize RNRs and viral RNAs in the early infection stage and to understand the mechanisms that allow viruses to uncoat into naked viral RNA and to replicate.

We have provided several lines of evidence indicating that Riplet complements RIG-I-mediated IFN-β induction upon viral infection by both Riplet siRNA and overexpression analyses. The C-terminal lysines (849 and 851) of RIG-I are critical for Riplet-mediated RIG-I ubiquitination. However, our data indicate that Riplet alone was unable to induce IFN-β production and essentially required RIG-I to confer IFN-β induction. Furthermore, Riplet is not ubiquitously distributed over the organs tested. Ubiquitination of RIG-I induced by poly(I-C) or viruses was accelerated in cells pre-transfected with Riplet. Hence, Riplet works case-sensitive to upregulate RIG-I antiviral activity predominantly in some organs. The physiological meaning of this response will be clarified by knockout study.

Unexpectedly, the siRNA experiments were not robust with regard to VSV replication. Possible explanations for this are as follows: 1) the degree of gene silencing is not so profound that the proteins remain in the cells; 2) there are a number of virus-mediated IFN-inducing pathways capable of compensating each other, so that disruption of one factor does not cause a profound effect on VSV replication. Furthermore, in VSV-infected Riplet-knockdown cells, IFN-β levels were reduced even at m.o.i. = 1 (Fig. 3*D*), and accordingly, virus susceptibility was increased at m.o.i. = 0.1 (Fig. 4*C*), whereas in Riplet-overexpressing cells, antiviral activity was observed only at low m.o.i. (Fig. 4*B*). We used different transfection reagents and cell conditions in the knockdown and overexpression experiments to obtain high transfection efficiency in each. These conditional differences in knockdown and overexpression analyses might cause part of the discrepancy between the two results on Riplet antiviral activity. Another possibility to explain the apparent inconsistencies between overexpression and knockdown analyses is that high amounts of Riplet efficiently activate the RIG-I signaling, but low amounts are insufficient for RIG-I activation in high m.o.i.-infecting human cells. High amounts of Riplet with overexpressed RIG-I would confer the ability on cells to respond to very low amounts of VSV as observed in the low m.o.i. experiments. Again, *riplet* knock-out mice would reveal whether it is absolutely required for potential RIG-I activation.

How viral RNAs select RIG-I rather than dicers or the translation machinery is also unknown. During natural infection it is likely that the number of the initial invading virions would be at most several copies/cell. Uncoated viral RNA may assemble a complex consisting of viral and host molecules required for replication. We assume that cells are equipped with various

molecular arms to sensitively detect viral RNA. The molecular complexes sensing viral RNA may not be so simple that we will be able to identify more molecules than Riplet as enhancers for integral RNA recognition. In either case, yeast screening will be a good strategy to pick up such proteins in other RNA recognition systems. A molecular switch selecting IFN induction by virus RNA will then be clarified.

We show that the ubiquitination sites targeted by Riplet are the helicase and RD domains of RIG-I but not its CARD-like domains in contrast to TRIM25. Riplet may be a complement factor of the reported TRIM25 function for RIG-I activation (23). A previous report (25) failed to polyubiquitinate the RIG-I protein by TRIM25 alone. If Riplet were added to TRIM25 for RIG-I ubiquitination in the previous study, Riplet would have enabled TRIM25 to polyubiquitinate the RIG-I CARD-like region. Further studies using TRIM25 and Riplet will be required to clarify this point.

Based on our results, we propose that RIG-I-like receptors form a molecular complex that efficiently recognizes low copy numbers of viral RNA. Riplet is implicated in the RIG-I complex to enhance viral RNA response in some organs. In this context, MDA5-associated molecules might also exist in the cytoplasm to augment IFN output. Although MDA5 possesses the RD domain, it fails to recruit Riplet (data not shown) or augment IFN-β-induction in conjunction with Riplet (Fig. 2*E*). Because RLR-associated molecules naturally reside in cells and facilitate inhibition of low dose viral infection until RLRs become expressed, they may be useful therapeutic targets for an early phase antiviral immunotherapy.

Acknowledgments—We thank Dr. M. Sasai in our laboratory for technical instructions for assay of RIG-I functions and Drs. K. Shimotohno (Keio University), T. Taniguchi (University of Tokyo), and T. Fujita (Kyoto University) for their critical discussions.

REFERENCES

1. Takeuchi, O., and Akira, S. (2008) *Curr. Opin. Immunol.* **20,** 17–22
2. Honda, K., Takaoka, A., and Taniguchi, T. (2006) *Immunity* **25,** 349–360
3. Kato, H., Takeuchi, O., Sato, S., Yoneyama, M., Yamamoto, M., Matsui, K., Uematsu, S., Jung, A., Kawai, T., Ishii, K. J., Yamaguchi, O., Otsu, K., Tsujimura, T., Koh, C. S., Reis e Sousa, C., Matsuura, Y., Fujita, T., and Akira, S. (2006) *Nature* **441,** 101–105
4. Venkataraman, T., Valdes, M., Elsby, R., Kakuta, S., Caceres, G., Saijo, S., Iwakura, Y., and Barber, G. N. (2007) *J. Immunol.* **178,** 6444–6455
5. Yoneyama, M., Kikuchi, M., Matsumoto, K., Imaizumi, T., Miyagishi, M., Taira, K., Foy, E., Loo, Y. M., Gale, M., Jr., Akira, S., Yonehara, S., Kato, A., and Fujita, T. (2005) *J. Immunol.* **175,** 2851–2858
6. Yoneyama, M., Kikuchi, M., Natsukawa, T., Shinobu, N., Imaizumi, T., Miyagishi, M., Taira, K., Akira, S., and Fujita, T. (2004) *Nat. Immunol.* **5,** 730–737
7. Hornung, V., Ellegast, J., Kim, S., Brzozka, K., Jung, A., Kato, H., Poeck, H., Akira, S., Conzelmann, K. K., Schlee, M., Endres, S., and Hartmann, G. (2006) *Science* **314,** 994–997
8. Pichlmair, A., Schulz, O., Tan, C. P., Naslund, T. I., Liljestrom, P., Weber, F., and Reis e Sousa, C. (2006) *Science* **314,** 997–1001
9. Saito, T., Hirai, R., Loo, Y. M., Owen, D., Johnson, C. L., Sinha, S. C., Akira, S., Fujita, T., and Gale, M., Jr. (2007) *Proc. Natl. Acad. Sci. U. S. A.* **104,** 582–587
10. Kawai, T., Takahashi, K., Sato, S., Coban, C., Kumar, H., Kato, H., Ishii, K. J., Takeuchi, O., and Akira, S. (2005) *Nat. Immunol.* **6,** 981–988
11. Meylan, E., Curran, J., Hofmann, K., Moradpour, D., Binder, M., Bartenschlager, R., and Tschopp, J. (2005) *Nature* **437,** 1167–1172
12. Seth, R. B., Sun, L., Ea, C. K., and Chen, Z. J. (2005) *Cell* **122,** 669–682
13. Xu, L. G., Wang, Y. Y., Han, K. J., Li, L. Y., Zhai, Z., and Shu, H. B. (2005) *Mol. Cell* **19,** 727–740
14. Rothenfusser, S., Goutagny, N., DiPerna, G., Gong, M., Monks, B. G., Schoenemeyer, A., Yamamoto, M., Akira, S., and Fitzgerald, K. A. (2005) *J. Immunol.* **175,** 5260–5268
15. Loo, Y. M., Fornek, J., Crochet, N., Bajwa, G., Perwitasari, O., Martinez-Sobrido, L., Akira, S., Gill, M. A., Garcia-Sastre, A., Katze, M. G., and Gale, M., Jr. (2008) *J. Virol.* **82,** 335–345
16. Komuro, A., and Horvath, C. M. (2006) *J. Virol.* **80,** 12332–12342
17. McWhirter, S. M., Tenoever, B. R., and Maniatis, T. (2005) *Cell* **122,** 645–647
18. Saha, S. K., Pietras, E. M., He, J. Q., Kang, J. R., Liu, S. Y., Oganesyan, G., Shahangian, A., Zarnegar, B., Shiba, T. L., Wang, Y., and Cheng, G. (2006) *EMBO J.* **25,** 3257–3263
19. Kayagaki, N., Phung, Q., Chan, S., Chaudhari, R., Quan, C., O'Rourke, K. M., Eby, M., Pietras, E., Cheng, G., Bazan, J. F., Zhang, Z., Arnott, D., and Dixit, V. M. (2007) *Science* **318,** 1628–1632
20. Lin, R., Yang, L., Nakhaei, P., Sun, Q., Sharif-Askari, E., Julkunen, I., and Hiscott, J. (2006) *J. Biol. Chem.* **281,** 2095–2103
21. Zhao, C., Denison, C., Huibregtse, J. M., Gygi, S., and Krug, R. M. (2005) *Proc. Natl. Acad. Sci. U. S. A.* **102,** 10200–10205
22. Arimoto, K., Konishi, H., and Shimotohno, K. (2008) *Mol. Immunol.* **45,** 1078–1084
23. Gack, M. U., Shin, Y. C., Joo, C. H., Urano, T., Liang, C., Sun, L., Takeuchi, O., Akira, S., Chen, Z., Inoue, S., and Jung, J. U. (2007) *Nature* **446,** 916–920
24. Urano, T., Saito, T., Tsukui, T., Fujita, M., Hosoi, T., Muramatsu, M., Ouchi, Y., and Inoue, S. (2002) *Nature* **417,** 871–875
25. Arimoto, K., Takahashi, H., Hishiki, T., Konishi, H., Fujita, T., and Shimotohno, K. (2007) *Proc. Natl. Acad. Sci. U. S. A.* **104,** 7500–7505
26. Sasai, M., Shingai, M., Funami, K., Yoneyama, M., Fujita, T., Matsumoto, M., and Seya, T. (2006) *J. Immunol.* **177,** 8676–8683
27. Douglas, J., Cilliers, D., Coleman, K., Tatton-Brown, K., Barker, K., Bernhard, B., Burn, J., Huson, S., Josifova, D., Lacombe, D., Malik, M., Mansour, S., Reid, E., Cormier-Daire, V., Cole, T., and Rahman, N. (2007) *Nat. Genet.* **39,** 963–965
28. Barral, P. M., Morrison, J. M., Drahos, J., Gupta, P., Sarkar, D., Fisher, P. B., and Racaniello, V. R. (2007) *J. Virol.* **81,** 3677–3684
29. Seol, J. H., Feldman, R. M., Zachariae, W., Shevchenko, A., Correll, C. C., Lyapina, S., Chi, Y., Galova, M., Claypool, J., Sandmeyer, S., Nasmyth, K., Deshaies, R. J., Shevchenko, A., and Deshaies, R. J. (1999) *Genes Dev.* **13,** 1614–1626
30. Pickart, C. M. (2004) *Cell* **116,** 181–190
31. Kim, M. J., Hwang, S. Y., Imaizumi, T., and Yoo, J. Y. (2008) *J. Virol.* **82,** 1474–1483
32. Alexopoulou, L., Holt, A. C., Medzhitov, R., and Flavell, R. A. (2001) *Nature* **413,** 732–738
33. Tanabe, M., Kurita-Taniguchi, M., Takeuchi, K., Takeda, M., Ayata, M., Ogura, H., Matsumoto, M., and Seya, T. (2003) *Biochem. Biophys. Res. Commun.* **311,** 39–48
34. Yoneyama, M., Suhara, W., Fukuhara, Y., Fukuda, M., Nishida, E., and Fujita, T. (1998) *EMBO J.* **17,** 1087–1095

Enhancement of antitumor natural killer cell activation by orally administered Spirulina extract in mice

Yuusuke Akao,[1,6] Takashi Ebihara,[1,6] Hisayo Masuda,[2,5,6] Yoshiko Saeki,[2] Takashi Akazawa,[2] Kaoru Hazeki,[3] Osamu Hazeki,[3] Misako Matsumoto[1,2] and Tsukasa Seya[1,2,4]

[1]Department of Microbiology and Immunology, Hokkaido University Graduate School of Medicine, Kita-15, Nishi-7, Kita-ku Sapporo 060-8638; [2]Department of Immunology, Osaka Medical Center for Cancer, Nakamichi 1-3-2, Higashinari-ku, Osaka 537-8511; [3]The Division of Molecular Medical Science, Graduate School of Biomedical Sciences, Hiroshima University, Minami-ku, Hiroshima 734-8551, Japan

(Received October 27, 2008/Revised April 6, 2009/Accepted April 8, 2009/Online publication May 6, 2009)

Oral administration of hot-water extract of Spirulina, cyanobacterium *Spirulina platensis*, leads to augmentation of NK cytotoxicity in humans. Here, we applied to syngeneic tumor-implant mice (C57BL/6 *versus* B16 melanoma) Spirulina to elucidate the mechanism of raising antitumor NK activation. A B16D8 subcell line barely expressed MHC class I but about 50% expressed Rae-1, a ligand for NK activation receptor NKG2D. The Rae-1-positive population of implant B16 melanoma was effectively eliminated in the tumor mass progressed in mice. This antitumor activity was induced in parallel with IFN-γ and abolished in mice by treatment with asialoGM-1 but not CD8β Ab, suggesting the effector is NK cell. NK cell activation occurred in the spleen of wild-type mice medicated with Spirulina. This Spirulina-mediated enhanced NK activation was abrogated in MyD88 –/– mice but not in TICAM-1 –/– mice. The NK activating properties of Spirulina depending on MyD88 were confirmed with *in vitro* bone marrow-derived dendritic cells expressing TLR2/4. In D16D8 tumor challenge studies, the antitumor effect of Spirulina was abolished in MyD88 –/– mice. Hence, orally administered Spirulina enhances tumoricidal NK activation through the MyD88 pathway. Spirulina exerted a synergistic antitumor activity with BCG–cell wall skeleton, which is known to activate the MyD88 pathway via TLR2/4 with no NK enhancing activity. Spirulina and BCG–cell wall skeleton synergistically augmented IFN-γ production and antitumor potential in the B16D8 *versus* C57BL/6 system. We infer from these results that NK activation by Spirulina has some advantage in combinational use with BCG–cell wall skeleton for developing adjuvant-based antitumor immunotherapy. (*Cancer Sci* 2009; 100: 1494–1501)

The immune system has innate and acquired arms to eliminate foreign cells from the host. The innate system recognizes pathogenic microbes which possess pattern molecules serving as ligands for pattern-recognition receptors.[1] These receptors reside in immune competent cells and trigger signaling to activate transcription factors in these cells.[2] Many cytokines and cellular effectors are consequently induced to orchestrate host defense. We have a variety of foods that may contain many kinds of microbial patterns. Since intestinal and colon epithelial cells express pattern-recognition receptors,[3,4] mucosal immune responses may be modulated by oral uptake of microbial material.

The cyanobacterium *Spirulina platensis* (Spirulina) has been taken as a supplemental food for more than 15 years without any undesirable side-effects.[5] Its safety for human consumption has been confirmed through toxicological studies.[5] Spirulina contains a lipopolysaccharide (LPS)-like constituent that structurally differs from the bacterial LPS.[6] Spirulina also contains high contents of protein, vitamins (especially A and B12) and minerals. It is rich in phenolic acids, tocopherols and γ-linolenic acid.[5,7] Since Spirulina lacks cell walls, it is easily digested.[7] Spirulina contains unique proteins, sugars and lipids[5,8] and these moieties of Spirulina are reported to participate in raising host immune responses including enhancement of Ab production,[9] cytokine liberation,[10] T-cell response and NK activation.[11] However, the exact molecular base responsible for these immune responses has not been clearly identified yet.

We previously reported that hot-water extract of Spirulina when taken orally in adult human enhances NK activation.[11] This Spirulina activity is unique since most of the reported bacterial adjuvants facilitate CTL induction but not NK activation.[12] For example, BCG–cell wall skeleton (CWS) subcutaneously injected induces IL-12, IFN-γ and local skin erosion but no NK activation.[13] TLR2 and TLR4 on myeloid dendritic cells (DCs) sense the peptidoglycan (PGN) of BCG (BCG–PGN) and induces DC maturation via the MyD88 pathway.[13,14] BCG–PGN drives DCs to elicit a CTL-inducing state.[15]

Here we show that hot-water extract of Spirulina activates NK in mice even by oral administration. Ingestion of Spirulina confers both IFN-γ production and NK-mediated Rae-1-positive cell killing activity in mice. Consequently, Spirulina administration leads to retardation of implant tumor growth in mice. This Spirulina antitumor activity depends on MyD88 but not the other adaptor TICAM-1 (TRIF). Thus, Spirulina evokes a unique MyD88-dependent NK activation through mucosal immune responses. We offer a possible immune therapy of BCG–CWS in combination with Spirulina in this communication.

Materials and Methods

Reagents and antibodies. The following materials were obtained: fetal calf serum (FCS) from Bio Whittaker (Walkersville, MD), mouse granulocyte–macrophage colony-stimulating factor (GM-CSF) and mouse IL-2 (mIL-2) from PeproTech EC, Ltd (London, UK), polymyxin B and lipopolysaccharide (LPS) (*Escherichia coli* O111:B4) from Sigma-Aldrich (St. Louis, MO), synthetic macrophage-activating lipopeptide 2 (MALP-2) from Amersham Pharmacia Biotech (Piscataway, NJ) and Lympholyte-M from Cedarlane (Ontario, Canada). Enzyme-linked immunosorbent assay (ELISA) kits for mouse (m)IFN-γ were obtained from Amersham Biosciences.

The following antibodies were used: antimouse NKG2D polyclonal Ab and antipan-Rae-1 polyclonal Ab (rabbit serum)

[4]To whom correspondence should be addressed.
E-mail: seya-tu@pop.med.hokudai.ac.jp
[5]Present address: Research and Education Center for Genetic Information, Nara Institute for Science and Technology, Ikoma, Nara 631-0101, Japan.
[6]These authors contributed equally to this work.

doi: 10.1111/j.1349-7006.2009.01188.x

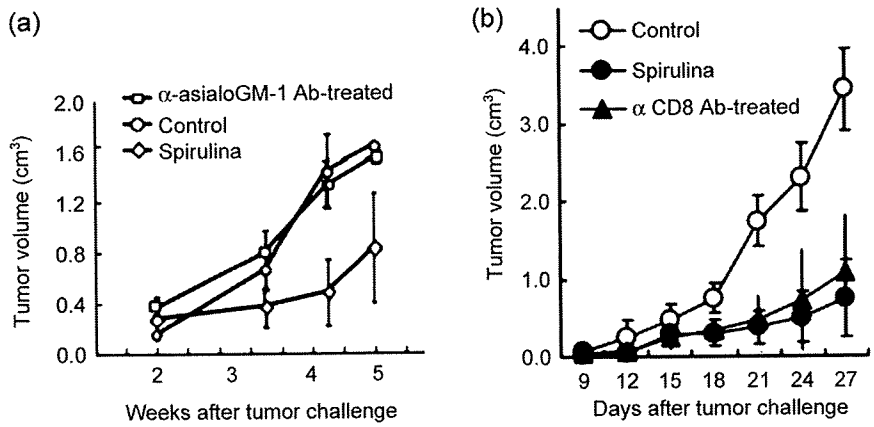

Fig. 1. AsialoGM-1 Ab-sensitive retardation of MHC-low tumor growth by oral administration of Spirulina. (a) Spirulina induces antitumor NK activation. C57BL/6 mice were separated into three groups ($n = 8$): one pretreated with anti-asialoGM-1 Ab and two with control saline, and except one control, fed with Spirulina from day 0, when B16 D8 subline was s.c. inoculated. Tumor volume was measured at intervals described in the Methods and statistical analysis was performed as described.[15] One mouse with saline only and one mouse given Spirulina and anti-asialoGM-1 Ab died of tumor after 5 weeks. We applied statistical analysis to seven live mice at the 5-week point of the two groups and declared the significance ($P < 0.05$). Represent mean ± SD. (b) CD8+ T-cells barely participate in Spirulina-mediated retardation of tumor growth. Wild-type C57BL/6 mice were grouped ($n = 5$). Spirulina extract (600 μg/600 μL) (●, ▲) or control saline (○) was orally administered to mice every other day from day −14. One group (▲) was pretreated with anti-CD8β Ab as described in the text. Then, B16D8 cells (6×10^5/head) were subcutaneously inoculated into the mice at day 0. Tumor volume was measured at indicated intervals until day 27 when the mice still survived. We declared the significance ($P < 0.05$) through statistical analysis.[15]

were established in our laboratory[16] and anti-asialoGM-1 Ab was obtained from Seikagaku Kogyo Co., Ltd. or Wako Pure Chemical Industrials, Ltd (Tokyo, Japan). Monoclonal Abs against mouse CD4 and CD8β were kindly provided by Drs T Takahashi and K Tsujimura (Aichi Cancer Center, Nagoya, Japan) as previously described.[17] Fluorescein isothiocyanate (FITC)-conjugated goat antirabbit and rat IgG $F(ab')_2$ were obtained from American Qualex (San Clemente, CA), rat IgG1κ control FITC from BD PharMingen (San Diego, CA), and hamster IgG isotype control FITC from eBioscience (San Diego, CA).

Preparation of BCG–CWS and hot-water extract of Spirulina. Spray-dried powder of *Spirulina platensis* propagated under basic conditions (pH 11) in outdoor open tanks was extracted with water in an autoclave for 1 h at 120°C. In some experiments, citric acid was added to the hot water extract to adjust the pH to 4.0.[18] The water-soluble extract was prepared by removal of insoluble fractions by centrifugation. The Spirulina extract was added to the mouse food at 1 mg/g (Clea Japan, Tokyo). In other experiments to administer accurate amounts of the extract to mice, the soluble extract of Spirulina was condensed to 1 mg/mL for oral administration as described previously.[18] In *in vitro* experiments, Spirulina extract was treated with polymyxin B (final concentration, 5 μg/mL) for 1 h at 37°C before cell stimulation to exclude the effect of possible contaminating LPS.

BCG–CWS was prepared in Dr I Azuma's laboratory (Research Institute for Immunology, Hokkaido University) as described previously.[19] The lot used in this study (Lot 10-2) consisted of mycolic acid, arabinogalactan and peptidoglycan with greater than 97% purity, and LPS contamination less than the detection limit (data not shown). Since BCG–CWS is insoluble in water and organic solvents, the oil-in-water emulsion form of BCG–PGN micelles (BCG-emulsion) was used throughout the *in vivo* study. B16 cell debris conjugated to BCG–CWS (BCG–CWS/Ag) was prepared as described below and detailed elsewhere.[15]

Mouse and cell lines. TLR2 −/−, TLR4 −/− and MyD88 −/− mice were gifts from Dr S Akira (Osaka University, Osaka) as previously reported.[15] TICAM-1 (TRIF) −/− mice were established in our laboratory.[17] Female C57BL/6 mice were purchased from Clea Japan. Mice were maintained in our institute under specific pathogen-free conditions. All animal work was performed under guidelines established by the Osaka Medical Center Institutional Animal Care and Use Committee. Mice (12-week-old female C57BL/6) were housed four per cage and allowed food and water *ad libitum*. Animal studies were carefully performed without ethical problems. In some experiments, mice were fed for 3 weeks with pathogen-free food containing 1 mg/g Spirulina extract and control food with no Spirulina, which were prepared by Clea Japan. For more precise studies 600 μg/head of the Spirulina extract was directly administered to the mouse stomach via an injector.

The B16D8 cell line was established in our laboratory as a subline of the B16 melanoma cell line.[20] This subline was characterized by its low MHC levels with no metastatic properties when injected s.c. into syngeneic C57BL/6 mice.[16,21] These cell lines were cultured in RPMI 1640/10% FCS. Tumor challenge studies were performed as previously described.[15]

Preparation of BMDCs and spleen NK cells of mice. Mouse bone marrow-derived DCs (BMDCs) were prepared as described previously.[15] Spleen NK cells were prepared by a reported method[22] with minor modifications.[23] In brief, spleen cells were passed through a nylon wool column to remove B-cells. In some cases, anti-asialoGM-1 Ab (100 μg) was injected intravenously into mice to eliminate NK cells.[17] The nylon wool-nonadherent cells were incubated in tissue culture plates for 1 h to remove adherent cells. Nonadherent cells were subjected to the MACS system (Miltenyi Biotec, Auburn, CA) for the preparation of NK cells.[23] The population was used as NK cells within 3 days.

Immunization. On days −28, −21, −14, −1 and +7 relative to the day of B16D8 challenge (Fig. 1), 5×10^6 B16D8 cells (in 90 μL) were in freeze–thaw cycles three times in PBS to prepare 'debris' and the debris was mixed with 10 μL of 1 mg/mL BCG–CWS in emulsion buffer (BCG–CWS/Ag).[15] Wild-type mice (>12 weeks old) were s.c. immunized with 30 μL of this mixture per head at the base of the tail. The administration protocol is shown in a previous report.[15] As controls, either tumor debris (Ag) only or emulsion only was used. Since BCG–CWS alone in emulsion buffer possesses immune potentiation activity upon subcutaneous (s.c) administration,[15,18] it could not be used as control for BCG–CWS/Ag.

Tumor challenge. B16D8 cells (2×10^6 cells in Fig. 1) were s.c. inoculated in the hind flank of wild-type mice. One group of

the mice was i.v. injected with anti-asialoGM-1 Ab (100 μg/100 μL) every week and the other was with mouse IgG. The tumor-challenged mice were fed with Spirulina-containing food from day 0 to the end of the study. In the next experiments, B16D8 cells (5×10^5 cells) were s.c. inoculated into mice, either preimmunized or non-immunized with BCG CWS/Ag. Mice were grouped into four, each consisting of 20 mice: group 1 with BCG–CWS/Ag and Spirulina, group 2 with BCG–CWS/Ag only, group 3 with Spirulina only and group 4 with no adjuvant. Likewise, mice were i.v. injected with anti-asialoGM-1 or anti-CD8β Abs (100 μg/100 μL) every week,[17] challenged with B16D8 and fed with Spirulina (600 μg/600 μL) every other day. The tumor sizes were compared with those of control mice. Tumor volumes were measured at regular intervals using a caliper. Tumor volume was calculated using the formula: Tumor volume (cm^3) = (long diameter) × (short diameter) × (short diameter) × 0.4.

Statistical analysis. A Student's *t*-test was used to examine the significance of the data when applicable in animal studies. Comparisons with more than two groups were done using ANOVA with appropriate *post hoc* testing. Differences were considered to be statistically significant when $P < 0.05$.

ELISA, flow cytometric (FACS) analysis of cell surface antigens. The levels of IFN-γ were determined by sandwich ELISA (Amersham Pharmacia Biotech, Buckinghamshire, UK) or the message levels assessed by quantitative PCR.[23] The practical methods for FACS were described previously.[24]

Quantitative RT-PCR. BMDCs were harvested 4 h after treatment with Spirulina extracts (50 μg/mL). The total RNA was extracted by RNeasy mini kit (Qiagen, Bothell, WA). Total RNA (0.5 μg) was incubated at 70°C for 5 min and then kept on ice for 2 min, and RT was performed as described previously.[25] The following primers were used for quantitative PCR: IFN-β forward, 5′-CCAGCTCCAAGAAAGGACGA-3′, and reverse 5′-CGCCCTGT AGGTGAGGTTGA-3′; IP-10 forward 5′-GTGTTGAGATCATT GCCACGA-3′, and reverse 5′-GCGTGGCTTCACTCCAGTTAA-3′. β-Actin was used as an internal control to normalize reactions.

Assessment of in vitro cytolytic activity. The cytolytic activity of spleen NK cells was determined by ^{51}Cr assay as described previously.[23] Effector lymphocytes were prepared from the spleen of intact C57BL/6 mice. A B16 subline (D8) or YAC-1 was used as a target cell. Target cells (0.4×10^4 cells/well) were co-incubated with the effector splenocytes at the indicated lymphocyte to target (E/T) cell ratio (typically 1, 5 and 20) in V-bottomed 96-well plates in a total volume of 200 μL of 0.5% BSA/RPMI-1640 medium at 37°C. Four hours later, the liberated ^{51}Cr in the medium was measured using a scintillation counter. Specific cytolytic activity was obtained by the formula: Specific cytotoxic activity (%) = [(experimental ^{51}Cr activity – spontaneous ^{51}Cr activity)/(total ^{51}Cr activity – spontaneous ^{51}Cr activity)] × 100. Each experiment was done in triplicate to confirm reproducibility of the results, and representative results are shown. A Student's *t*-test was used to examine the significance of the data.

Results

Tumor regression in mice given Spirulina. Retardation of tumor growth was observed in implant B16D8 tumor in mice when given Spirulina. The suppression of tumor growth by Spirulina was abrogated if the mice were treated with anti-asialoGM-1 Ab to eliminate NK cells[17] (Fig. 1a). The effect of Spirulina on tumor regression was somewhat variable in a mouse-to-mouse fashion, but was significant ($n = 8$). The mouse group with Spirulina all survived 6 weeks after tumor challenge although some died in the control and NK-depleted groups by 6 weeks. The results were confirmed with additional experiments, where NK activation occurred in mice in response to being fed Spirulina and disrupted by administration of anti-asialoGM-1 Ab (data not shown). We further confirmed that depletion of CD8+ T-cells had virtually no effect on Spirulina-mediated antitumor activity (Fig. 1b). NK activation may have occurred in mice given Spirulina to retard tumor growth.

NK activation in mice given Spirulina. We confirmed that the hot-water extract of Spirulina induces NK activation by direct NK assay. Mice (wild-type) were orally administered with the extract of Spirulina or just saline (control) every other day for 2 weeks. The NK fraction of the spleen cells was prepared by MACS beads and cultured *in vitro* in medium only (Fig. 2a). NK-mediated cytotoxicity was determined using an NK-target, YAC-1. NK activation was enhanced in the group with Spirulina compared to those without Spirulina (Fig. 2a). Similar results were obtained with the B16D8 cells as targets (data not shown). We next tested what molecular mechanisms participate in the Spirulina-mediated NK-enhanced activation. We used MyD88 –/– and TICAM-1 –/– mice to test the Spirulina NK-enhancing effect (Fig. 2b). In MyD88 –/–mice NK activation was not enhanced by administration of Spirulina, while in TICAM-1 –/– mice NK activation was enhanced by Spirulina as in wild-type mice. Hence, the TLR pathway involving MyD88, but not TICAM-1, participates in NK activation. NK cytotoxicity was already high in control mice given no Spirulina, irrespective of disruption of the TLR pathways (Fig. 2b), suggesting that other factors than TLRs also participate in *in vivo* NK activation. We found that BMDCs prepared *in vitro* elicit NK-enhancing activity in response to the extract of Spirulina (Fig. 2c,d). The ability of Spirulina to drive NK activation in BMDCs was not abrogated with TICAM-1 –/– BMDCs but abrogated with MyD88 –/– BMDCs (Fig. 2d). Consistent with the result that MyD88 rather than TICAM-1 is crucial for Spirulina-mediated NK activation by BMDC, TICAM-1-dependent mediators IFN-β and IP-10 were barely induced in Spirulina-stimulated BMDCs (Fig. 2e). Our interpretation of these results is that part of the *in vivo* NK-enhancing activity by Spirulina is attributable to the MyD88 pathway in BMDCs resulting in BMDC–NK reciprocal activation. Using this *in vitro* system, we tested if TLR2 and TLR4 are involved in the Spirulina NK-enhancing activity. TLR2/4-double deficient mice severely abrogated the response to Spirulina to reduce the Spirulina-mediated NK enhancing activity (Fig. 2c), although either one of TLR2 or 4 deficiency exhibited only a marginal effect on NK-enhancing activity by Spirulina. Thus, TLR2/4 and MyD88 participate in Spirulina-mediated BMDC-NK activation.

Additive tumor regression by BCG–CWS and Spirulina. BCG–CWS is an agonist of TLR2/4 to activate the MyD88 pathway, but does not activate NK cells,[12,13] in contrast to the Spirulina extract. MyD88 may have two arms to drive CTL and NK cells in this context. BCG–CWS/Ag subcutaneously administered effectively matures antigen-presenting dendritic cells to induce tumoricidal CTL depending upon antigens selected.[15] We next checked whether BCG–CWS/Ag and Spirulina elicit a synergistic effect on tumor regression in B16D8 melanoma-bearing mice (Fig. 3a). In this experiment, tumor burden was controlled for mice to survive greater than 6 weeks after tumor challenge. Four mouse groups ($n = 20$ each) were made to test if the tumor suppression activity depended on the host response to BCG–CWS/Ag and/or Spirulina in the same B16 implant system. Although either BCG–CWS/Ag or Spirulina alone exerted ability to regress the implant tumor, the combination of both most effectively reduced tumor sizes ($P < 0.05$) (Fig. 3a). Thus, Spirulina and BCG–CWS/Ag additively suppress tumor progression. Survival rate of mice challenged with B16D8 is also shown in Fig. 3(b). The group treated with BCG–CWS and Spirulina survived the longest, since 45% of mice in this group were alive after 9 weeks, by the time more than 80% of control mice died. Mice treated with anti-asialoGM-1 Ab all died by 9 weeks (Fig. 3b), suggesting the importance of NK cells for antitumor immune response and long survival.

doi: 10.1111/j.1349-7006.2009.01188.x

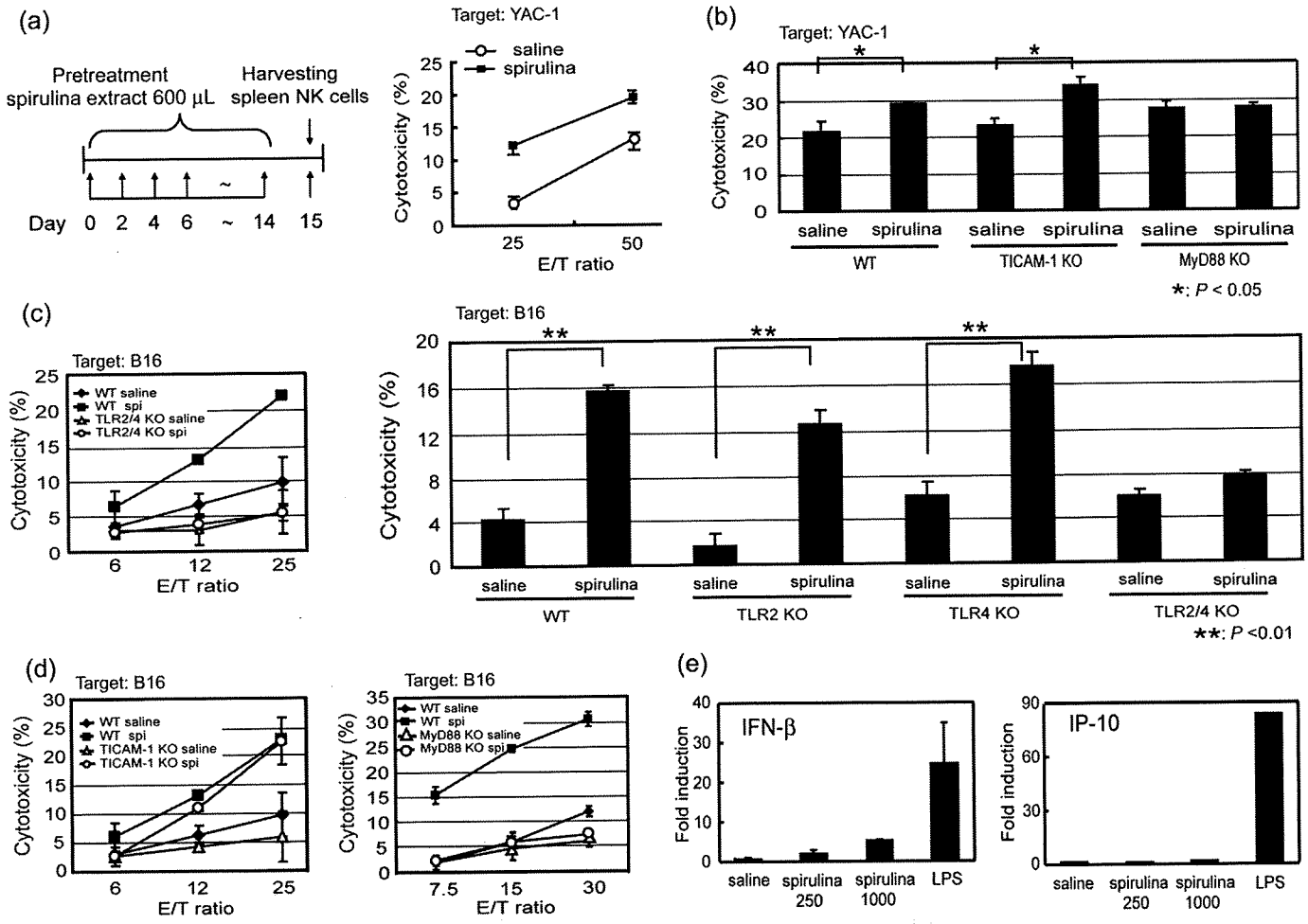

Fig. 2. Orally administered Spirulina enhances NK activation in mice. (a) YAC-1 killing activity of spleen NK cells harvested from mice with or without Spirulina. Spirulina extract (600 μg/600 μL) was orally administered into mice every other day. Two weeks later, spleen cells were harvested to isolate NK cells by MACS beads from wild-type mice. NK activity against YAC-1 or B16D8 cells (not shown) were determined at the indicated E/T ratio. (b) Participation of MyD88 in enhanced NK activation by Spirulina. NK cells were prepared from wild-type, TICAM-1 –/– or MyD88 –/– mice which had been treated with saline or Spirulina extract as in (a). NK cytotoxic activity was determined using YAC-1. (c) Spirulina effect on BMDC-NK activation was abrogated with TLR2/4 –/– BMDCs. BMDCs from wild-type and TLR2/4-double deficient mice were stimulated with Spirulina extract for 4 h and mixed with NK cells for 24 h. The mixture was incubated with ^{51}Cr-labeled target B16 cells for 4 h at the E/T ratio indicated (left panel). In the right panel, BMDCs of the indicated KO mice were admixed with NK cells as in the left panel. NK activity was determined using ^{51}Cr-labeled B16 target at a fixed E/T ratio (1:25). Percentage cytotoxicity was determined as in (a). Only slight abrogation of the Spirulina-mediated NK activation was observed in either TLR2 –/– or TLR4 –/– BMDCs under the same conditions (data not shown). (d) Spirulina acts on BMDC and augments MyD88-mediated NK reciprocal activation by BMDC. BMDCs with TICAM-1 –/– (left panel) and MyD88 –/– (right panel) were stimulated with Spirulina extract for 4 h and mixed with NK cells for 24 h. The mixture was incubated with ^{51}Cr-labeled target B16 cells for 4 h at the E/T ratio indicated. Percentage cytotoxicity was determined as (a). (e) The mRNA levels of IFN-β and IP-10 in BMDCs were determined by quantitative PCR 4 h after Spirulina stimulation. These experiments were performed three times and similar results were obtained. Representative analyses are shown.

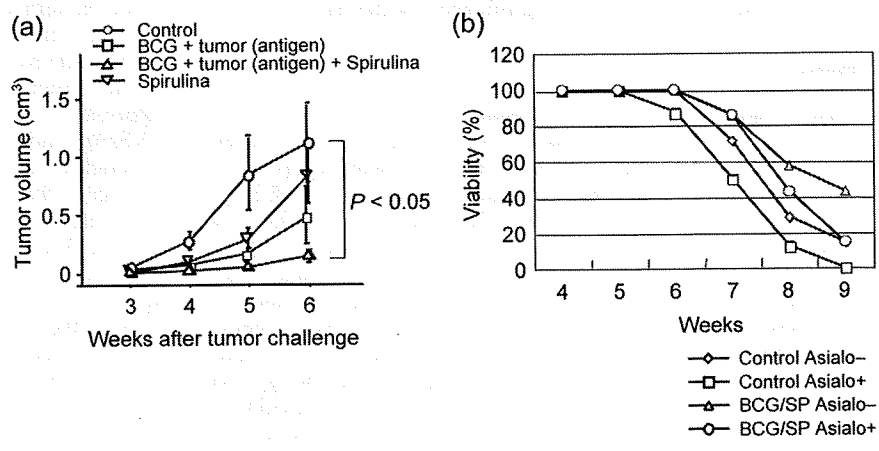

Fig. 3. Implant tumor retardation by BCG–CWS and Spirulina in mice. (a) C57BL/6 mice were separated into four groups (n = 20): group 1 with saline only, group 2 with BCG–CWS/B16 Ag, group 3 with Spirulina and group 4 with BCG–CWS/Ag and Spirulina. BCG–CWS/Ag was administered four times from day –21 to day 0,[15] while Spirulina was fed from day –21 to the end of the survey (see inset). B16D8 subline was s.c. inoculated at day 0. Tumor volume was measured at intervals and statistical analysis was performed as described.[15] (b) Mice were grouped into four (n = 20) as indicated in (a), and the effect of asialoGM-1 Ab on the survival of tumor-implant mice was analyzed. The survival rate was plotted for each group of mice.

Levels of IFN-γ in Spirulina/BCG–CWS-treated mice. IFN-γ is an effector that may be associated with prognosis of patients with BCG–CWS adjuvant immunotherapy.[26] IFN-γ was secreted in the blood of mice with tumor burden if they were treated with BCG–CWS and Ag (Fig. 4). Either BCG–CWS/Ag or Spirulina alone slightly induced IFN-γ. The levels of IFN-γ induced by Spirulina appeared low in mice compared to human volunteers.[11] Tumor antigen had no effect on the level of Spirulina-mediated IFN induction (data not shown). Notably, significantly high levels of IFN-γ were detected in mice treated with both BCG–CWS/Ag and Spirulina (Fig. 4). Skin reaction reflecting BCG hypersensitivity was observed in the relevant group (data not shown). No or less skin reaction was observed in the group with BCG–CWS/Ag and Spirulina. Spirulina alone did not induce skin reaction.

Rae-1-positive B16 cells were eliminated by Spirulina. B16D8 cells in implant tumor of C57BL/6 mice consisted of Rae-1-positive and -negative cells. The cells were inoculated into the mice which were fed and/or treated with the material indicated (Fig. 5). Implanted B16 tumor cells were extracted from the tumor-bearing mice 5 weeks after tumor challenge, stained with the indicated Abs and analyzed by FACS (Fig. 5), where mean fluorescence intensities are shown in the insets. In the group given no Spirulina, tumor cells consisted of Rae-1-positive and -negative populations, whereas in the group given Spirulina, the Rae-1-positive population was selectively diminished. The group treated with Spirulina and anti-asialoGM-1 Ab possessed the Rae-1-positive population. Other markers including MHC class I and class II were neither detectable nor different among the groups. Although other NK-activation ligands were detected in message levels, they still remained in the Rae-1-negative cells (data not shown). Thus, Rae-1-positive tumor cells are selectively eliminated by Spirulina-derived NK cells in this mouse system.

This issue was confirmed using an *in vitro* assay. NK cells reciprocally activated by Spirulina-treated BMDCs damaged B16D8 cells (Fig. 6a). The NK-mediated B16D8 killing was largely blocked by the addition of anti-NKG2D Ab (Fig. 6a).

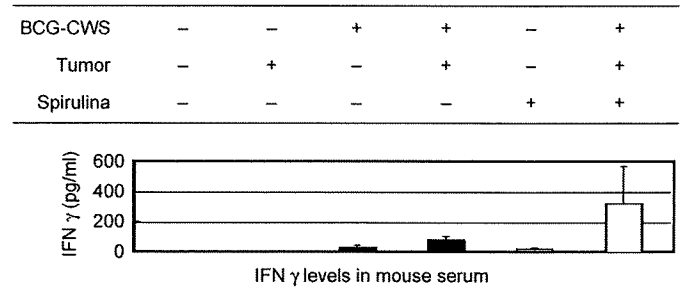

Fig. 4. Serum level of IFN-γ in tumor-bearing mice given BCG–CWS and/or Spirulina. Mice were treated with BCG–CWS/B16 Ag and/or Spirulina and inoculated with B16 tumor at day 0 as in Fig. 3. Forty-eight hours after tumor implantation, mouse sera were obtained from their tails and the levels of IFN-γ were determined by ELISA.

Without BMDCs, Spirulina extract treatment barely activated NK cells (data not shown). Thus, NK-mediated B16D8 killing was attributable to interaction between tumor cell Rae-1 and NK cell NKG2D, which is supported by Spirulina-dependent maturation of BMDC, as there is no direct route for Spirulina-mediated NK activation.

Spirulina-mediated B16D8 growth was largely abrogated in MyD88 –/– mice (Fig. 6b). Antitumor NK activation predicted in this study may occur in tumor-bearing mice through being given Spirulina.

Discussion

We demonstrated that tumor growth is retarded in mice given Spirulina. Unique points in this study are: (i) Rae-1-positive tumor cells are selectively eliminated in Spirulina-fed mice; and (ii) marked tumor regression is observed in mice with combinational administration of BCG–CWS/Ag and Spirulina. Synergistic effects on tumor regression and increase of serum

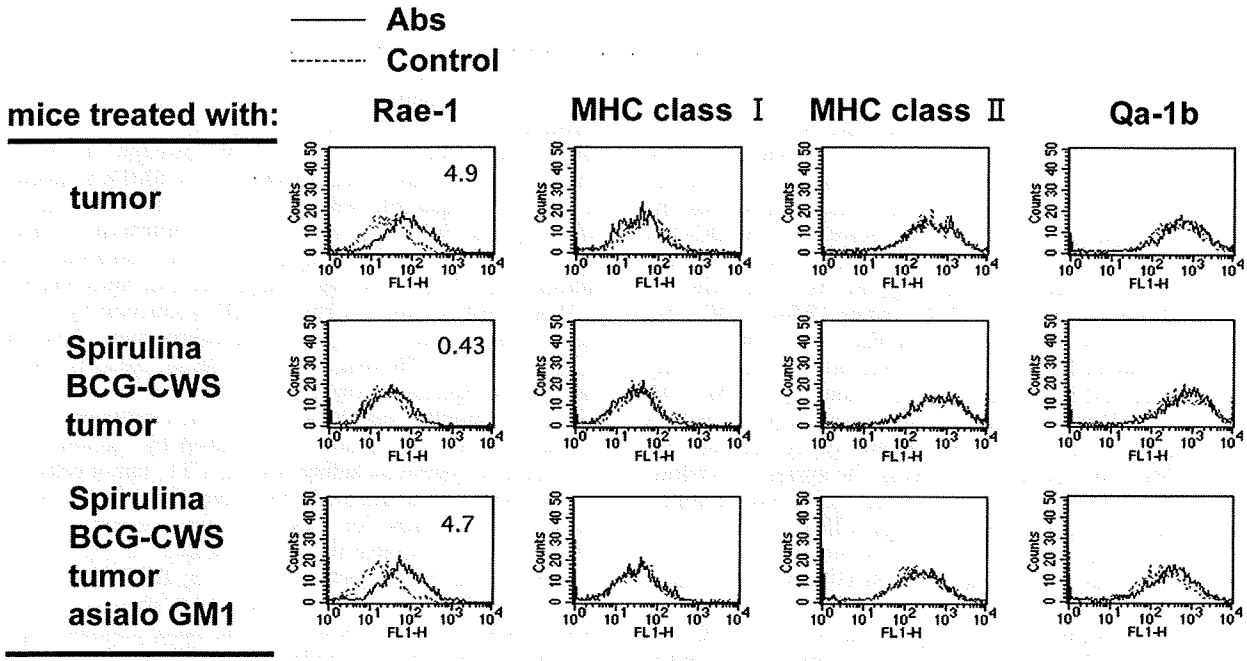

Fig. 5. Rae-1 and MHC levels in the implant tumor of mice. Mice were treated with anti-asialoGM-1 Ab, Spirulina, B16 tumor Ag and/or BCG–CWS as in Fig. 3, and inoculated with B16 cells; prescriptions are indicated in the left column. Five weeks later, the cells were harvested and dispersed in PBS–EDTA. The levels of Rae-1, MHC class I, MHC class II and Qa-1b were assessed by FACS using their specific Abs.[16] Specific mean fluorescence intensities of Rae-1 are indicated in the fluorograms as described elsewhere.[16]

doi: 10.1111/j.1349-7006.2009.01188.x

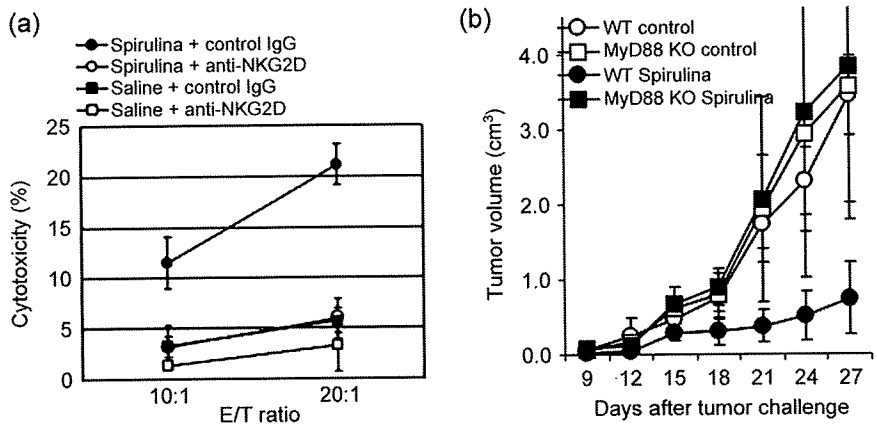

Fig. 6. Spirulina NK cells damage B16D8 tumor cells through MyD88 and NKG2D receptor. (a) NK cells kill B16D8 cells through NKG2D after incubation with Spirulina-treated BMDCs. BMDCs from wild-type mice were stimulated with Spirulina extract for 4 h and mixed with NK cells for 24 h (DC:NK = 1:3). The mixture was incubated with anti-NKG2D Ab or control IgG and ^{51}Cr-labeled target B16 cells for 4 h at the E/T ratio indicated. (b) MyD88 is crucial for Spirulina-mediated tumor growth retardation. Wild-type and MyD88 –/– mice were grouped as shown. Spirulina extract (600 μg/600 μL) (●, ■) or control saline (○, □) was orally administered to wild-type and MyD88 –/– mice (n = 5) every other day from day –14. B16D8 cells (6×10^5/head) were subcutaneously inoculated into the mice at day 0. Tumor volume was measured at indicated timed intervals until day 27 when the mice survived, and statistical analysis was performed as in Fig. 1 ($P < 0.05$).

IFN-γ level were observed in mice by combination treatment with BCG–CWS/Ag and Spirulina. BCG–CWS/Ag induces CTL via TLR2/4 in myeloid DCs in a MyD88-dependent manner.[15] In this study, Spirulina activates NK cells also via TLR2/4 in BMDCs in a MyD88-dependent manner. These reports suggest that simultaneous attack by CTL and NK more effectively regresses tumor cells in mouse tumor implant models.

Our *in vitro* findings on Spirulina allowed us to interpret that the Spirulina extract activates the MyD88 pathway in BMDCs to evoke activation of mouse NK cells (Fig. 2). What mechanisms activate the MyD88 pathway to drive NK cells in Spirulina-stimulated BMDCs is an intriguing issue, since other TLR2/4 ligands mainly engage CTL induction, but not NK activation, via the MyD88 pathway in BMDCs.[27,28] Difference in downstream signal events may cause the different outcomes of NK/CTL induction in BMDCs. Studying the Spirulina-activated MyD88 pathway will be an important issue to clarify how it is possible to have two TLR2/4 agonists activate NK and CTL.

There appear several routes for activation of NK cells. The BMDC-mediated NK activation serves an important route for NK-mediated tumor clearance.[29–31] We demonstrated that the TICAM-1 (TRIF) pathway in BMDCs participates in the DC–NK reciprocal activation.[17,27,32] In contrast, most of the non-DNA/RNA adjuvants currently available originate from bacteria and activate the MyD88 pathway of TLR2 and/or TLR4 in DCs, but they barely induce NK activation.[17,28] In this context, BCG–CWS expressed high tumor-killing activity (Fig. 3a), but this activity was barely abrogated by administration of anti-asialoGM-1 Ab (data not shown). Further, Spirulina appears to differ from LPS in its adjuvant activity, since LPS simultaneously activates the MyD88 and TICAM-1 pathways to evoke the systemic cytokine storm. The Spirulina extract is unique because it has an ability to activate NK cells without inducing type I IFNs.

Spirulina-mediated IFN-γ production is greatly enhanced in mice by simultaneous administration of BCG–CWS/Ag, similar to humans.[33] How Spirulina participates in IFN-γ production is a future question. Spirulina ultimately activates T- and NK cells in mice, although IFN-γ is poorly induced in mice compared to human volunteers with only Spirulina.[11] Direct addition of Spirulina to splenic lymphocytes neither results in NKG2D up-regulation nor induces enhanced B16D8 cell killing (data not shown), suggesting that cell populations other than DCs in the spleen barely participate in this event. There is a report that the MAPK pathway of BMDCs participates in promotion of NK activation by BMDCs.[34] If this is the case, the NK-enhancing effect by Spirulina in human patients can be evaluated in the mouse model and IFN-γ production is a good marker for NK activation.

Previous studies on patients with cancer suggested that Spirulina constituents serve as protective agents against oral cancers[35] in terms of tumor progression and metastasis,[36] although the results are from non-randomized trials. These reports were reminiscent of the antitumor functions of Spirulina, some of which would be derived from β-carotene, an effective antioxidant.[37] Indeed, the serum levels of β-carotene are consistently low in patients with cancer.[37,38] Our present study may offer additional evidence that NK activation is a representative of the Spirulina-mediated antitumor immunity.

However, a point remains unsettled that the constituents of Spirulina taken up via the intestine and colon do not always correspond to those of the extract of Spirulina. *In vitro* studies where Spirulina was added to NK cells or BMDCs appear not to be simply comparable with the *in vivo* studies using mice. In other reports, Spirulina orally taken significantly reduced IL-4 levels in individuals with allergic rhinitis by a randomized double-blinded trial.[39] Another report suggested that Spirulina enhances IgG1 and IgA production but not IgE production by modulating the mucosal immune system.[9] Spirulina may skew the Th2 polarization to a Th1-like state in allergic patients. We should identify the Spirulina constituents associated with activation of mucosal immunity and absorbed into the circulation.

Since cancers are usually established by circumventing the host immune system including NK and CTL, tumor cells generally possess poor immunogenicity by expressing low levels of MHC class I and ligands for NK-activating receptors including NKG2D.[40] It is notable that these receptor levels are regulated by IFN-γ. It has been reported that during BCG adjuvant therapy the increased serum level of IFN-γ 18 h after s.c. injection of BCG–CWS is a marker for evoking the innate immune response.[26] In mouse experimental models using syngeneic transplantable tumors, MHC class I-expressing tumor cells were selectively eliminated by BCG–CWS/Ag s.c. injection,[15] and the serum levels of IFN-γ were increased in the case of Spirulina, too. Nevertheless, tumor cells with low MHC expression remain,